An Affordable Particle Detector for Education

Brendan James Arnold

May 12, 2005

Contents

Acknowledgements

An Affordable Particle Detector for Education has proved to be a stimulating and highly enjoyable project. I would like to thank the following people who have made it so.

I would like to thank my lab partner for bringing the project together and for bringing me down to Earth, Dr. Cussans for being helpful and enthusiastic, John 'the glass' Rowden for opening the door on the wonderful world of glass, Richard 'safety guy' Exley for keeping us alive, Dave Milson, Bob Sadler and the rest of the guys in the workshop for help and advice (both academic and extra curricular) and Jerry Hart for running around after us, wisdom and banter.

I would also like to thank the people on the IOP PNTC mailing list and TES forums for the survey results as well as help in gathering information. Finally I would like to acknowledge the SDF Public Access UNIX facility whose facilities I used to typeset this report and develop the computer models.

Abstract

This project continues ongoing work done at Bristol University researching an affordable, safe particle detector to be used as experimental apparatus in 'A Level' education. In particular we investigated Resistive Plate Chambers (RPCs). Much work was done on the resistive electrode coatings including studies of long-term drying and application to float glass. We built a working prototype although further refining needs to be done due to low signal to noise ratios of around 9.5dB. We estimate the cost of a very basic RPC detector could be driven as low as £75 per unit.

1 Introduction

Now in its third year at Bristol University as an undergraduate project[1], *An Affordable Particle Detector for Education* seeks to bring the physics of cosmic rays and other high energy particles to secondary school classrooms. This year we have two projects running in parallel, one continuing work of previous years into scintillator detectors[1] and ours which explores a promising new avenue into budget ionisation chambers.

All main UK A-Level syllabus[2] feature particle physics at some point. Commercially available particle detectors seem to be restricted to cloud chambers and although there are relatively cheap [2] ones available, they need a source of dry ice, a resource that we estimate less than half of UK schools have access to (see research undertaken in section 2). A further problem with cloud chambers is that data is difficult to log. Although a video camera arrangement can be used, this is relatively costly in terms of equipment and requires time-consuming human analysis to get results. This also closes off the possibility of collaborative experiments such as the Swedish SEASA project where particle detectors from different schools are linked into a huge detector array[3] which is potentially valuable in terms of research.

We chose to investigate Resistive Plate Chambers (RPCs), a derivative of the spark chamber. An RPC works in much the same way as a spark chamber but does not require triggering with costly supplemental detectors, moreover the materials used for construction (largely Soda-lime float glass) are readily and cheaply available. Due to their low cost, RPCs are often used in high energy physics to detect muons, the most penetrating, charged component of many collisions. Muon detectors are often found in the extreme outer perimeter of general purpose detectors and therefore make up a large part of the bulk. Although inexpensive in terms of materials, typical RPCs used in industrial applications are largely unsuitable for classroom use. There are three major factors that need to be remedied:

1. The majority of RPC designs involve very high voltages, up to 10kV and beyond, much greater than the 1–2kV needed to operate photomultiplier tubes (PMTs) in scintillator detectors and also much greater than the 5kV limit on secondary school high voltage supplies recommended by CLEAPSS[3].

2. Gas mixtures used in RPCs are often flammable, largely due to the Butane or Isobutane quencher and also often use highly greenhouse

[1]See projects of the same name by J. Miles & S. Townrow in 2004 and L. Ainsbury & B. Motz in 2003

[2]Fisher Scientific supply a Cloud Chamber kit in the US for *$60.45* [Cat. No: S52008]

[3]*Consortium of Local Education Authorities for the Provision of Science Services*, see `http://www.cleapss.org.uk/`

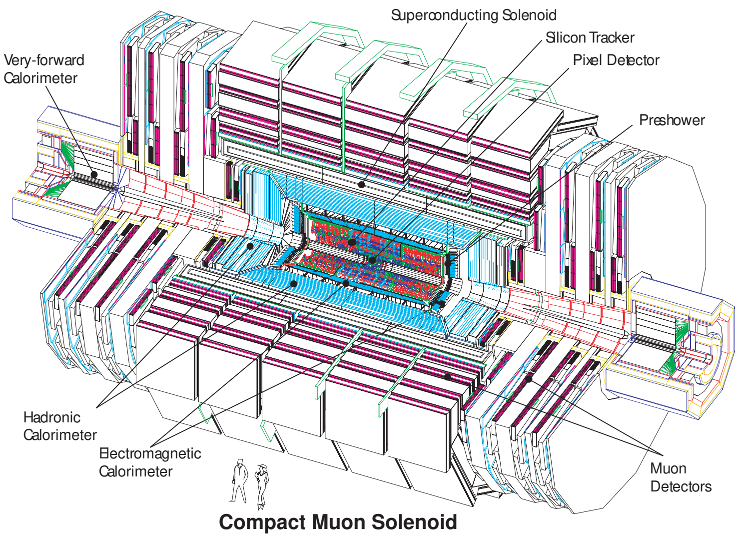

Figure 1: CMS Detector at CERN, RPCs detect the muons near the outer perimeter[4]

gases such as Freon 134-a and Sulphur Hexafluoride. Schools are going to want to be seen to be as safe and as environmentally aware as possible.

3. Most RPC applications have a through flow of gas. For cosmic ray experiments this would mean frequent replenishing of the canisters, escalating the cost to the point where most schools would not be able to afford the units.

Fortunately RPCs are highly adaptable, there already exists research which has investigated lower voltage (< 5kV) designs with high efficiencies[30] as well as research into non-flammable, freonless gas mixtures[5]. The through flow of gas is to prevent premature ageing of detectors[6] although research has been undertaken which suggests that glass is ageing resistant[7]. A chamber wholly made of glass with no electrodes exposed to the gas within should age well, prompting us to believe a ‘sealed for life’ unit is feasible.

2 Preliminary Work

An online survey was undertaken early in the year to determine some parameters with which we could work within. The questions were chosen in order to get a better picture of the level of interest in the project, what facilities schools had (in terms of equipment and budget) and what kind of detector was wanted as a teaching tool. The following is from a result set of 35 physics teachers in the UK teaching between GCSE and A-Level education. Full details of the method employed in the survey as well as the entire results set is found in Appendix A.

2.1 Detector budget

Figure 2 shows a cumulative histogram of what schools can afford. It shows a sharp drop which gradually levels out, suggesting that most schools, unsurprisingly, have a relatively low budget. 55% of schools can afford £100–£150 however 50% can afford £150–£200 which is a relatively small drop. subsidies of up to £100 bring this within reach of 75% of schools. Therefore our budget should either be £150–£200 with up to £100 subsidies or simply £50–£100.

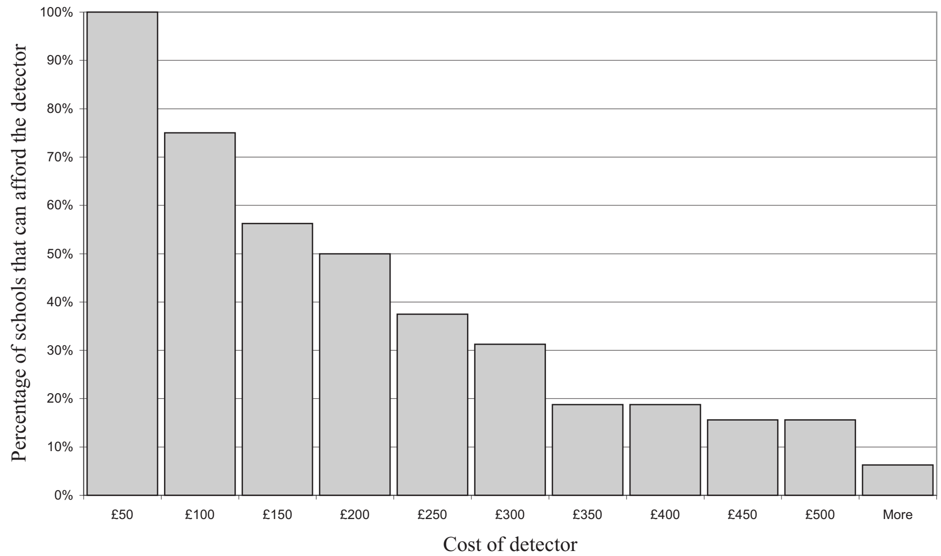

Figure 2: Cumulative histogram plot of what schools can afford for a detector

2.2 School facilities

In determining the feasibility of our project, we see that nearly 70% of schools already have access to power supplies of 4kV or over (most are in fact 5kV) which could represent considerable saving on the RPCs and any detector involving photomultiplier tubes. All schools have access to a PC making long-term result taking and collaborative arrays possible. We also see that almost all schools have access to a fume cupboard which could be used to house the RPCs in the interests of safety.

In previous years cloud chamber were considered. The survey shows that if we were to follow this route we would almost certainly have to supply a source of dry ice which would elevate the cost through CO_2 cylinder hire and compression equipment. However we see that over half the schools have access to a digital video camera making long term cloud chamber experiments possible.

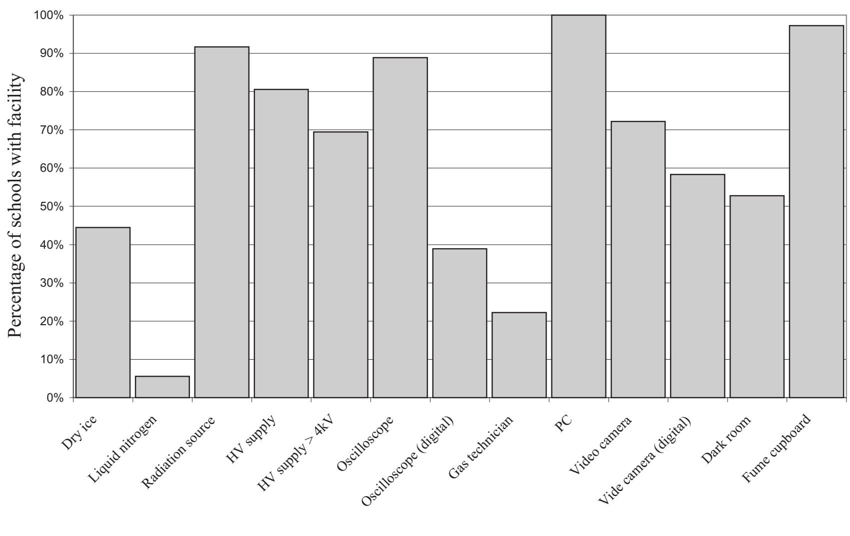

Figure 3: Facilities available to schools

2.3 Demonstration vs. investigation

Nearly half the teacher interviewed expressed that they would use the detector primarily for demonstration purposes, almost all the rest wanted it to be suitable for demonstration *and* investigation, only 8% wanted to use the detector for investigation purposes. This leans in favour of spark chamber and cloud chambers or other visual detectors which make the cosmic rays 'appear' in front of the students eyes. RPCs have been used in the past to photograph streamers[28] by using transparent electrodes and so it may be possible to make the final design a visual detector.

2.4 Collaborative array

Interest in participating in a collaborative array, similar to NALTA[10] in America and SEASA[3] in Sweden ranged from a minimum of 58% to a maximum of 92%, the large uncertainty margin made of people who specified 'maybe', most stating that it would have to be sufficiently automatic and not take up their time. This implies that if a collaborative array is decided upon, it would probably have to be remotely administered by someone at the university.

3 Theory

The scope of this project does not encompass actual study of cosmic rays, nor the breakdown of gas. The following treatment is written so as to give a basic understanding of what is happening in our detector as well as, in the case of extended air showers, some of its applications.

3.1 Cosmic Rays

Cosmic rays can be loosely defined as energetic particles which do not originate from Earth[8]. This encompasses many possible sources ranging from solar flares, to supernovae, to sources as yet unidentified for the extreme high energy cosmic rays. It also encompasses many types of particle ranging from heavy nuclei to electron neutrinos.

3.1.1 Cosmic rays in space

We categorise cosmic rays as either *primary* or *secondary*, primaries being the original particle that was created at the astrophysical source, secondaries being 'debris' particles created after a primary collides with some intervening matter in its passage across the cosmos. Particles produced in abundance by stars such as electrons, protons and helium, carbon, oxygen and iron nuclei are primaries, other nuclei are more likely to be secondaries. The Earth's atmosphere either absorbs or converts most primary particles into secondary particles (predominantly neutral and charged pions) before they get to sea-level, primary energies are important however since greatly affect our detected secondaries. Figure 4 shows the energy spectrum of the major components of primary cosmic rays.

The Earth is shielded somewhat both by the Sun and by its magnetic field. There is a reduction in flux of particles in primaries below 10GeV[9] that reach the top of the Earth's atmosphere.

3.1.2 Cosmic rays in the atmosphere

High energy primary cosmic rays collide with particles high in the atmosphere in deep inelastic collisions that cause jets of secondary hadrons, most of which are pions although more exotic mesons can be produced. The charged pions with a mean lifetime of 2.6×10^{-8} seconds decay to muons over 99.98% of the time whilst around 98.8% of neutral pions decay to photons[12] which then go on to trigger electromagnetic showers[4]. The end result is a shower of secondary 'debris' which consists chiefly of photons (80%)[5] and electrons (18%) from electromagnetic showers, muons (1.7%)

[4]For a more complete table of decay modes of pions see Appendix B

[5]Percentages are by particle numbers, source [3]

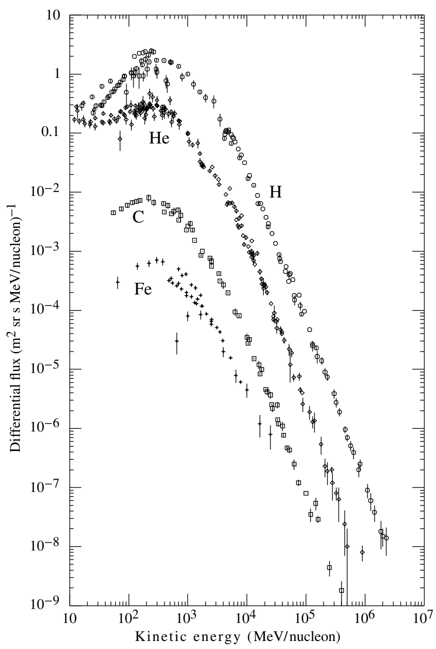

Figure 4: Primary cosmic ray energy spectrum at typical energies[13]

and muon neutrinos as well as nucleonic remnants (protons and neutrons) from the primary and other hadrons.

These *air showers*, or *extensive air showers* when they reach a large enough size, are highly significant since the area they cover and their angle is directly related to the energy of the primary particle which caused it. This provides us with a way of measuring ultra-high energy primary particle energies from Earth using relatively low cost arrays of small detectors. We envisage the possibility of designing our detector in such a way so that they could be used in such an array[6]. As a rule of thumb, there are around 1–1.6 particles in an EAS for each GeV of energy of the primary[11].

3.1.3 Muons

Figure 5 shows the vertical fluxes of the secondaries of $E > 1$GeV versus altitude. We see that on average muons are the most abundant charged particles to reach the surface with a vertical flux of around $90m^{-2}s^{-1}\mathrm{sr}^{-1}$.

The majority of particles we will be detecting are muons since they are both penetrating enough to reach ground through the atmosphere but are also ionising allowing us to use the most common particle detection techniques.

[6]For examples of similar existing projects, see references [3] and [10]

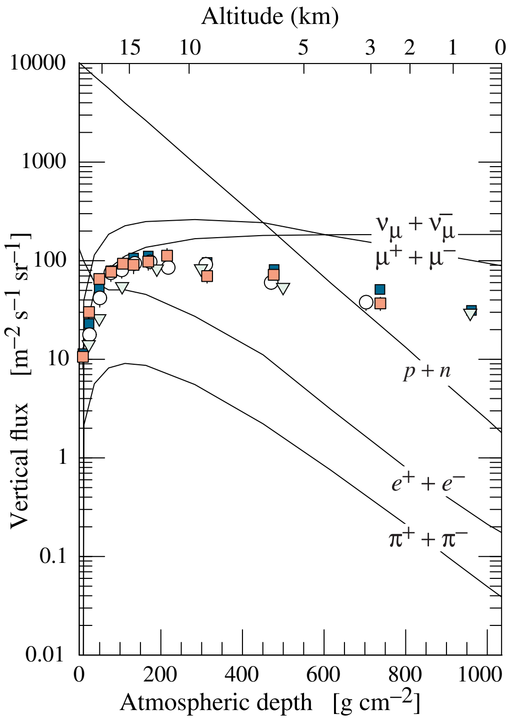

Figure 5: Cosmic rays in the atmosphere with energy greater than 1GeV[13]

The angular distribution of muons with $E \sim 3$GeV at ground level is $\alpha \cos^2 \theta$ where α is the vertical flux. For lower energies this steepens whilst at higher energies it tends towards $\alpha \sec \theta$ for muons with energy much greater than the pion critical energy and for $\theta < 70°$[13]. The mean energy of muons at ground is approximately 4GeV[13].

3.2 Depositing Energy

Most particle detectors rely on ionisation in order to detect charged particles, however, energy is deposited in other ways.

As a cosmic ray passes through matter, provided it is below a critical energy particular to each particle, E_c, it loses most of its energy through ionisation. Above E_c energy is lost through a radiative process known as *Bremsstrahlung*, particle-antiparticle pair production and photonuclear events. E_c for muons at 4GeV in various common gases used in RPCs are given in the table below[29].

Gas	Ionisn.	Bremms.	Pair prod.	Photonucl.	Total	E_c
			$MeV.cm^2.g^{-1}$			GeV
Air	2.396	0.001	0.001	0.002	2.401	1115
Argon	2.054	0.003	0.002	0.002	2.061	572
Butane	2.928	0.001	0.001	0.002	2.932	1557
Freon 12	2.008	0.002	0.002	0.002	2.014	615
CO_2	2.401	0.002	0.001	0.002	2.405	1095
Oxygen	2.054	0.003	0.002	0.002	2.061	1050

As you can see, by far the largest component of energy loss is due to ionisation for any of the gases at 4GeV. The critical energy is much higher than 4GeV for all listed gases.

3.2.1 Bethe-Bloche formula

The Bethe-Bloche formula describes the average stopping power ($\langle -dE/dx \rangle$) for energies where ionisation dominates,

$$-\left(\frac{dE}{dx}\right) = \left(\frac{4\pi N_A \alpha^2 (\hbar c)^2}{m_e}\right) z^2 \frac{\rho Z}{A} \frac{1}{\beta^2} \left[\frac{1}{2} \ln\left(\frac{2(\beta\gamma)^2 m_e T_{max}}{I^2}\right) - \beta^2 - \frac{\delta}{2}\right]$$

where N_A is Avagadro's number, α is the fine structure constant, m_e is the mass of an electron, z is the charge number of the absorber, ρ is density of the medium, Z is the atomic number of the absorber, A is the atomic mass of the absorber, I is the typical ionisation energy of the absorber atoms and δ is a correction applied for the density effect. The density effect is when a particle's electric field extends forwards at high energies increasing the amount of forward interactions, in practice polarisation limits this, hence

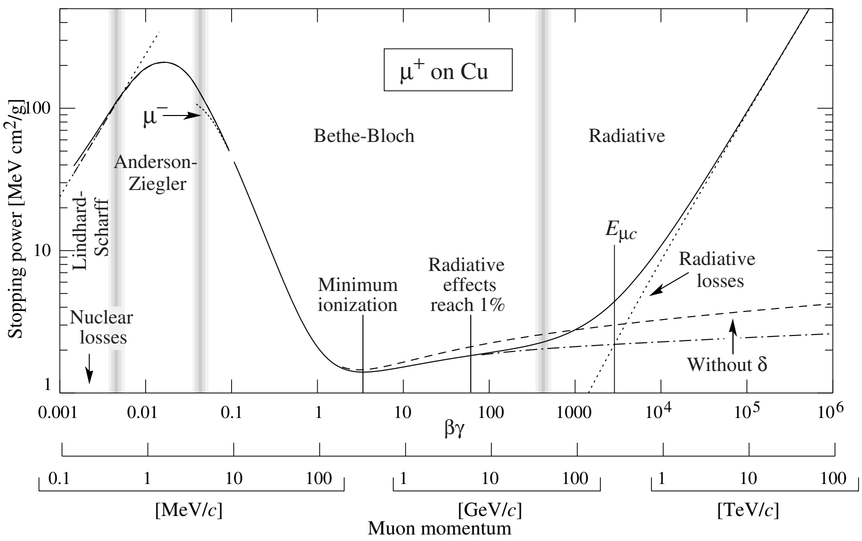

Figure 6: Stopping power for μ^+ passing through copper[13]

the correction term. T_{max} is the maximum amount of energy that can be given to an electron and is given by,

$$T_{max} = \frac{3m_e c^2 \beta^2 \gamma^2}{1 + 2\gamma m_e/M + (m_e/M)^2}$$

where M is the mass of the particle.

To find the rate of energy loss for mixtures of different absorbers, the rates for each component are multiplied by its proportion in the mixture and then summed. This is known as Bragg addivity.[14]

Figure 6 gives a fuller picture for particle energies above and below the Bethe-Bloche ionisation region. Although it is for positive muons in copper, the general shape is independent of the particle and the material it is passing through.

3.3 Electrical breakdown of gas

In various gas ionisation chambers the initial ionisation due to the passing particle is what is used to register a particle event. The ionisation is exploited in different ways by different detectors in the ionisation chamber family depending on which stage of the breakdown process is used to take measurements. The initial ionisation progresses to a continuous arc through the following steps,

$$\text{Ionisation} \rightarrow \text{Avalanche} \rightarrow \text{Streamer} \rightarrow \text{Spark} \rightarrow \text{Arc}$$

Typical amounts of charge released for each process along with typical voltages is shown in figure 7, although the voltages can be delayed by the addition of quenchers to the gas mixture (see section 4.4.1).

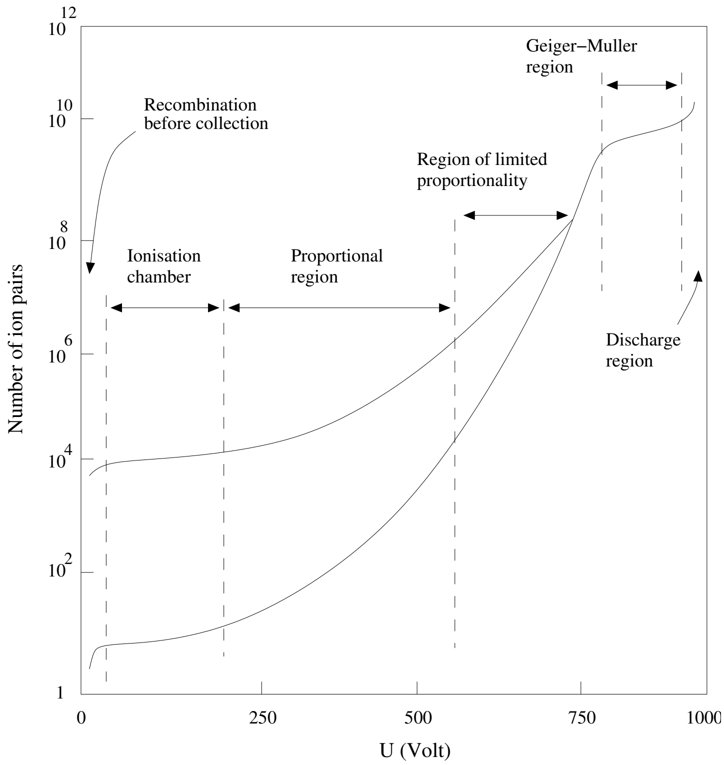

Figure 7: Charge release from discharge processes[15]. The lower line represents charge released from alpha particles, the upper line for electrons

3.3.1 Ionisation

The initial incident particle causes ionisation as it passes through the chamber. The particle must impart at least the first level *minimum ionising energy* of the atom in order to create an electron-ion pair. Using a weak electric field this initial ionisation can be gathered and measured but since this tends to be low (10s of electron-ion pairs) the signal is very weak and is only useful for large fluxes of particles, not for the single particle events such as cosmic rays. Detectors which rely on this alone are know simply as ionisation chambers.

3.3.2 Townsend avalanche

If after the initial ionisation there is a strong electric field present the electrons and ions accelerate towards the anode and cathode respectively. If the electrons are accelerated enough that they gain enough energy to impart the minimum ionising energy then they can cause further ionisation through collisions. The process continues into an electron avalanche known as a *Townsend avalanche*. The ions are not accelerated so much due to their massive size and so do not gain so much energy. Provided the avalanche

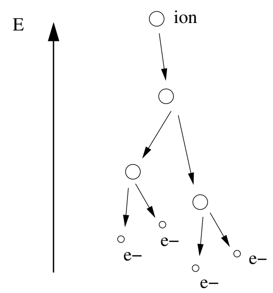

Figure 8: Townsend avalanche

does not get too large, the amount of charge is proportional to the initial ionisation. The gain in the number of electrons or *gas multiplication*, M, is given by,

$$M = e^{\alpha x}$$

Where x is the distance the avalanche has travelled and α is the inverse of the mean free ionisation distance of the gas or the *first Townsend coefficient*. Proportional and drift chambers use gas multiplication.

Once the avalanche has reached a certain size it starts to develop into a streamer. It create its own electric field which affects the growth of the avalanche. Here we have *limited proportionality* where the simple relationship no longer holds although it is still possible to calibrate the chamber to give initial energy deposited.

Many high-rate RPCs operate in 'avalanche' mode.

3.3.3 Streamers

The secondary field between the electrons in the head and the relatively immobile ions acts to counter the external field resulting in a net weakened field. In this region of conflicting fields the plasma (ion gas) begins to dissipate through recombination. As the pairs re-combine, they emit photons. Photons are not affected by the electric field and so are free to move in any direction. Those that move laterally cause photoelectric ionisation

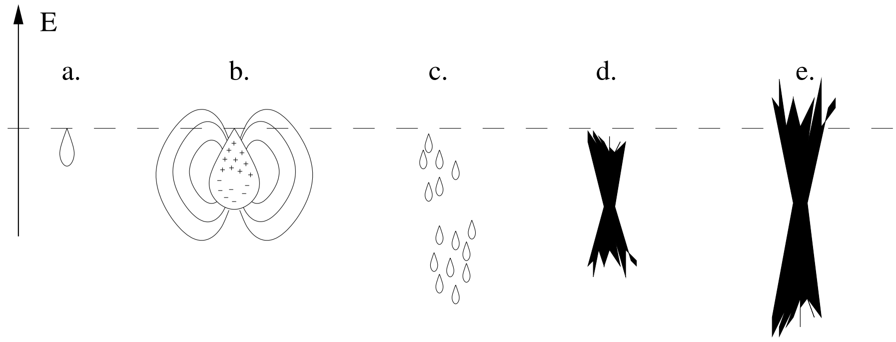

Figure 9: The development of a streamer in time[15]. (a) initial avalanche, (b) polarisation effects of avalanche – limited proportionality, (c) secondary avalanches due to photoionisation, (d) early streamer, (e) developed streamer

immediately alongside the main avalanche although further development is subdued due to the reduced electric field, those that ionise atoms above and below the main avalanche however cause avalanches of their own in the reinforced electric field. Eventually the avalanches meet and a continuous streamer channel is established which bridges the gas gap, paving the way for a spark.

Photons can also cause further avalanches and streamers elsewhere laterally in the chamber which is what happens in Geiger-Muller tubes. Discharges of this sort lose their spatial resolution, are unpredictable and result in long dead-times before the residual ions are cleared.

Streamers develop between 1-10mm in length, beyond this the leader process takes over[16].

3.3.4 Spark

Once the gas gap has been bridged by a streamer it can either dissipate or breakdown into a spark. When a spark bridges the electrodes, the charge in the spark no longer has any relation to the amount of ionisation initially released by the particle. Rather it is determined by the capacitance of the electrodes using the simple capacitor equation, $Q = CV$.

3.3.5 Arc

An arc is a continuing spark and occurs depending on whether the currently decaying plasma can sustain itself by conducting enough current to raise its temperature to the point where recombination ceases to occur. In air this has to occur in a few microseconds, in noble gases longer[16].

An arc, once established can continue indefinitely and act as a highly conductive channel. Arcs can only be sustained if the electrodes are continually replenished by a high voltage supply. The current in an arc is very high which is what heats the channel, ensuring the gas remains in a plasma state and remains conductive.

4 Resistive Plate Chambers (RPCs)

Resistive plate chambers use the ionisation principle to create signals, they operate in 'streamer' or 'avalanche' mode. Figure 10 shows a skeleton RPC design. An RPC comprises of two plates of highly resistive material (typ-

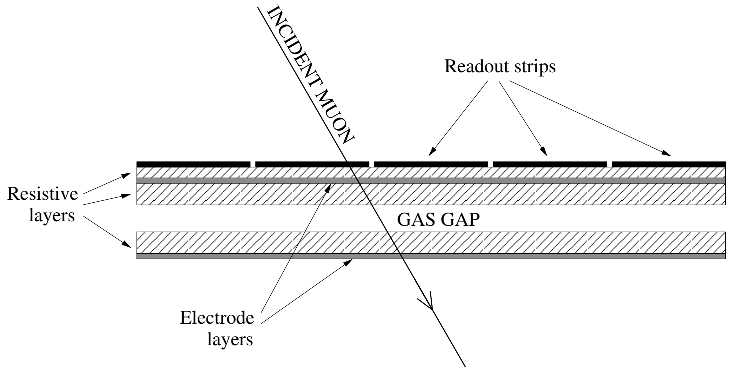

Figure 10: Schematic of a basic RPC

ically bakelite or float glass) which lie between the anode and cathode of medium resistivity (10^5–$10^7\,\Omega$/square), the plates in turn are separated by a small ($\sim$ 2mm) gas gap filled with a gas mix. A particle event is registered by readout strips of conducting material which lie outside of the electrodes.

As the name suggests, resistive plate chambers differ from other ionisation chambers due to the resistive plates. These offer protection against arcing and allow for an external readout circuit.

4.1 Resistive plates

With the resistive plates the discharge is no longer maintained after the initial arc due to the drop in voltage resulting from the high resistances. Figure 11 show how the spark discharge could be represented by a circuit diagram. We use Ohms Law to calculate the voltage across the plasma channel in a spark chamber and in an RPC.

$$\text{Spark Chamber:} \qquad V_{plasma} = V$$

$$\text{RPC:} \qquad V_{plasma} = \frac{V R_{plasma}}{(2R_{plate} + R_{plasma})} \approx \frac{V R_{plasma}}{2R_{plate}}$$

Since R_{plate} is typically very high ($\sim 10^{12} - 10^{16}\Omega/$ square for float glass) and R_{plasma} very low, V_{plasma} is greatly reduced. This brings the voltage across the plasma below the threshold for a sustained arc, thus suppressing the arc.

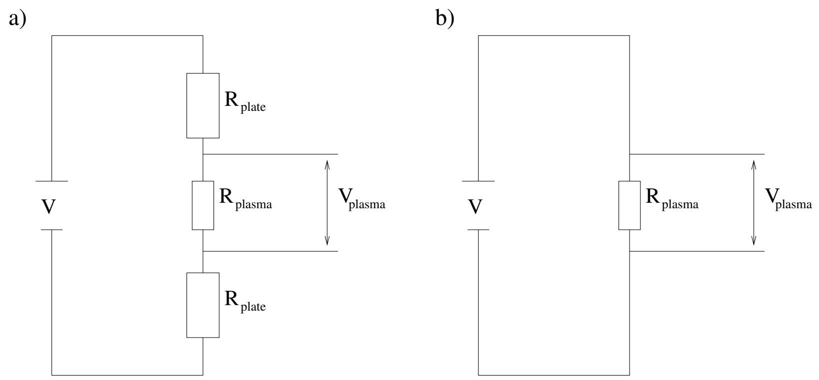

Figure 11: Equivelance circuit for discharge in (a) an RPC and (b) a spark chamber

4.2 Resistive electrodes

The electrodes are of a medium surface resistivity so as both conduct enough to apply the high voltage electric field to the gas but also be resistive enough (or 'transparent' enough) so that the charge pulse from the gas is localised at a particular point, see section 4.3.

Typically the resistive electrodes are a layer of graphite paint, ink, graphite tape or anti-static spray.

An extensive investigation into suitable resistive coatings was performed in section 5.4

4.3 Readout strips

The second advantage of the resistive plates is that it allows external read-out strips in a separate read-out circuit which rely on charge induction for readings. The resistive coating helps localise the charge before it is dissipated. Figure 12 shows an equivalence circuit for the readout-strips. The advantage of this over taking readings from electrodes are that it is not necessary to use high voltage capacitors to remove the high voltage DC for taking readings, it is less sensitive to any voltage ripples from the power supply and it allows for greater flexibility in readout design, in particular the perpendicular readout strips.

4.3.1 Perpendicular readout strips

To obtain an x-y readout where the readout is taken directly from the electrodes requires $n \times m$ readout channels, where $n \times m$ is the resolution. Using two sets of perpendicular strips however allows the same resolution with only $n + m$ readout channels, which represents a considerable saving in readout

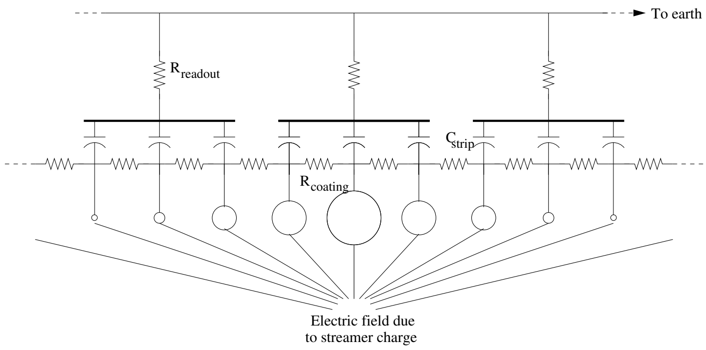

Figure 12: Equivalance circuit for readout strips and resistive electrode coating. The size of the circles indicates the magnitude of the charge reaching the HV electrodes (not to scale)[20]

electronics for high resolution applications.

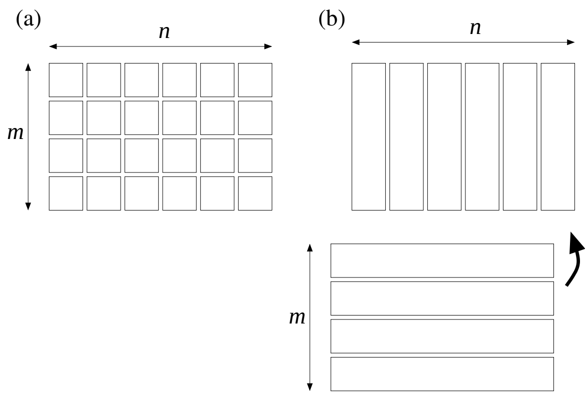

Figure 13: Grid arrangement in (a) only option for combined electrode and readout. Arrangement in (b) possible with induced readout on external strips

4.4 Gas mixtures

Gas mixtures are tailored to the application of the RPC. Townsend avalanches occur in weaker electric fields in noble gases than in molecular gases[6] and so it is common to find a noble gas as part of the gas mix. Generally this is Argon due to its low cost and because, unlike helium, it is relatively easy to contain. After this often an ultraviolet and electron *quencher* is needed to control the magnitude of the discharge in the chamber.

4.4.1 Quenchers

To prevent too much lateral spread of the avalanches as it develops into a steamer, often a quencher is added to the mixture of gases. This is usually a large molecular gas with lots of vibrational modes which can readily absorb the ultraviolet photons emitted in the streamer development process and/or a gas with an incomplete electron shell which can soak up excess electrons.

Typical examples of ultraviolet quenchers are isobutane and butane (H_4C_{10}), electron quenchers tend to be a freon of some sort, normally tetrafluorethane ($F_3C–CH_2F$)or sulphurhexafluoride (SF_6). Research has also gone into using gases with lower Global Warming Potentials (GWP)[5] such as oxygen and carbon dioxide[7].

4.4.2 Flammability

Typically mixtures include a significant proportion of the highly flammable butane. The 'magic mix', a mixture commonly used in multi-wire proportional chambers has 24.5% butane[6], some RPC mixes go as far as 50%[30]. The flammability limit is around 10% butane, any more than this and the mixture will burn in air. This is modified when oxygen is added to the mix[8]. In light of the fact that often sparks form across the gas in streamer mode RPCs and that we are envisaging a sealed unit which may over time leak air in, a non-flammable gas mix is essential for this project.

4.4.3 Effects of humidity

Studies have suggested that water vapour can reduce the efficiency of glass RPCs to 30%[19]. It also affects the glass resistivity significantly[18]. For this reason gas mixes may have to dried with silica gel crystals.

5 Building the RPCs

We decided upon a fairly standard RPC design with a few novel features. Firstly the chamber itself is built entirely of float glass. Glass has good chemical properties and is suitably resistive, Bristol University also has a glass workshop to hand. Secondly the gas is delivered through two glass tubes drilled into one of the plates (for our initial prototypes we need to be able to change the gas inside), which saves having to breach the fragile glass spacer frame, risking damage. Figure 14 shows the components of the central chamber.

[7]Tetrafluorethane has a GWP 1300 and SF_6 has a GWP $24,900$ times that of CO_2. Oxygen does not contribute at all.

[8]For a flammability curve of oxygen against carbon dioxide, see reference[5]

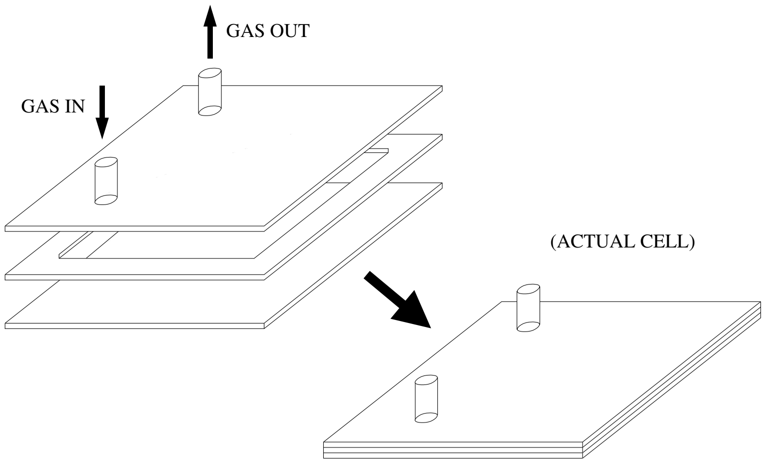

Figure 14: Construction of chamber using float glass frame

5.1 Gas mixing and delivery system

The gas delivery system served two purposes, firstly it allowed us to mix gases in various proportions, secondly it regulated the pressures of the gases into a more manageable pressure suitable for the RPC. The final arrangement featured a calibrated water tower composed of a lower and upper bell jar. Figure 15 demonstrates the setup, Each gas cylinder is connected and

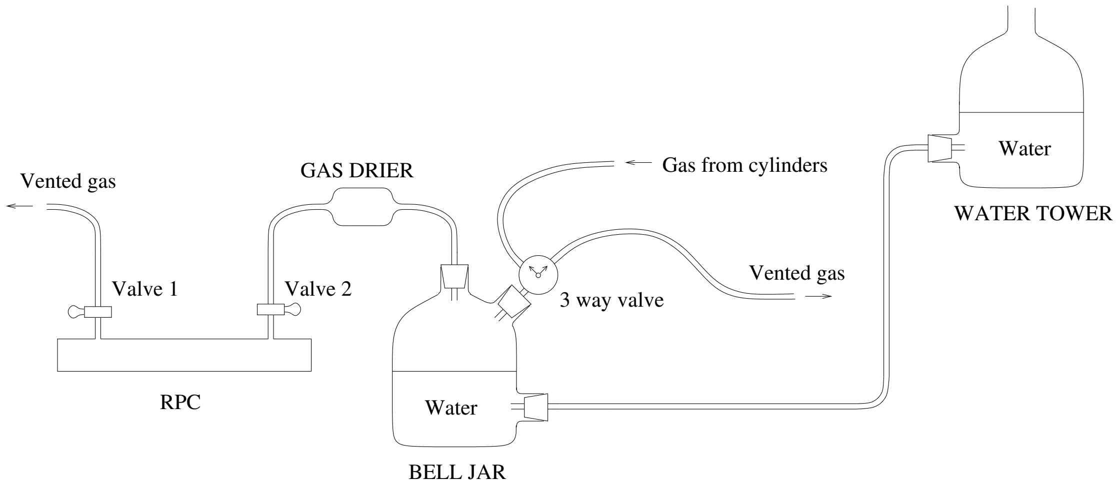

Figure 15: Schematic diagram of the gas mixing and delivery system

initially flushed through the tubing at the three way valve. Once confident that any residual gas has been flushed the gas is then redirected into the bell jar displacing the water into the upper bell jar. This is repeated for all gases. The delivery pipe is then isolated and the valves leading to the RPC are opened. The pressure of the water in the upper jar pushes the gas through at a reasonably steady pace.

We included a 'drier', a glass chamber filled with silica gel to keep the gas free from water vapour which can affect efficiency. This and all other components are connected by rubber piping making the entire setup modular making replacement of parts simple should something fail. The system was in theory standardised to 8mm width tubing, although in practice this was not possible due to availability of components. We tested for leaks by running the system through with Argon and using a solution of water and washing up liquid around the seals to look for bubbles. In the end we resorted to using silicon sealant to patch up leaks.

Originally we were going to measure the amounts of gas put into the jar using a set of scales under one of the bell jars and weigh the volume of water displaced. Knowing the density of water at room temperature we could calculate the volume of gas that had entered the system. However we could not get hold of a set of scales that could weigh amounts above the 5kg of water in the bell jar with suitable precision. Instead, we calibrated the lower bell jar by displacing the water into a large measuring cylinder, graduations were marked on in permanent ink. There were problems placing the water level through since the thick glass of the bell jar which meant that there was an parallax error in reading out. We estimate this error to be around 15ml.

5.2 Readout system

Since we planned on constructing several prototype chambers we decided to make one readout system which was easily interchangeable between chambers to save on materials and better compare the chambers themselves. This unit was dubbed 'Dave'.

The main readout panel was constructed of a sheet of single sided printed circuit board (PCB)[9]. This provided copper readout strips which we could etch to whatever pattern we chose as well as a 1.6mm layer of insulation in the form of the fibreglass substrate. We discovered the neatest way to remove narrow strips of copper on the board is to first score the track with a Stanley blade, then apply a soldering iron to melt off the glue, the strips should peel off.

Since we wanted to investigate the effects of the readout strip size and the localisation of the signal we etched a series of concentric rectangles as our readout strips, the measurements are shown in figure 16 the idea was that the gaps could be bridged with conducting tape to adjust the area of the readout plate. The readout signal was delivered through a BNC cable

[9]RS Part no. 433-927

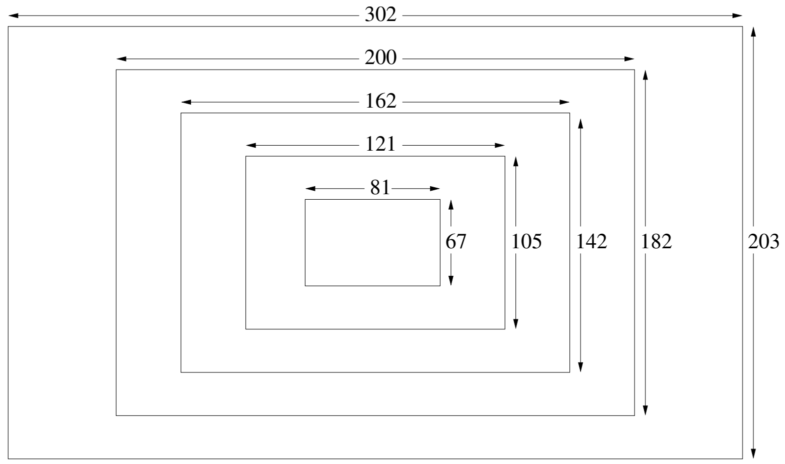

Figure 16: Dimensions of the readout plates

soldered onto the centre plate through the wooden clamping plate used to hold it all together. Any part of the PCB which was not used as readout, was connected to earth effectively providing electrical shielding from the high voltage resistive electrode beneath. The high voltage was delivered via a SHV cable which plugged into an earthed aluminium box on the earthed part of the PCB. The HV cable on the inside of the box followed a line of copper tape through to the bottom of the readout unit which was pressed against another strip of copper tape connected to the HV resistive electrode on each one of the chambers. See figure 17. In practice the connection did

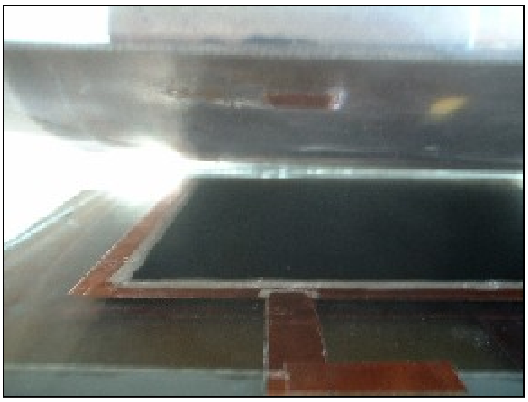

Figure 17: The HV join between the readout unit and the chamber

not quite make and so had to be forced together with a G-clamp.

5.2.1 Electronics

Initially we observed the signal from the readout plate directly through a digital oscilloscope[10] chosen for its high bandwidth capabilities since our signal would be of the order of a few nanoseconds in duration. We also experimented with 10 fold amplification via. a LeCroy nim crate unit[11]. Eventually we envisaged designing our own electronics circuit comprising of cheaper components. Although we did not get to this stage, there are several useful starting points online, in particular the SEASA project[3] features some rough circuit diagrams and appendix C shows a diagram used in the homebrew detector at cosmicrays.org.

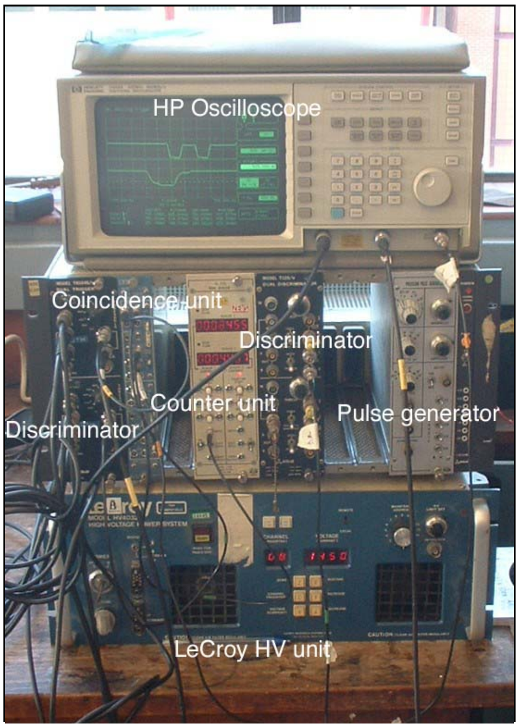

Figure 18: The electronics setup used in our experiment

5.3 High voltage system

The high voltage was supplied by a LeCroy HV4032A unit. This featured three removable pods, two which supplied up to +7kV and −7kV[12] the final

[10]HP 54502A, serial no. CRO 309 A718508

[11]LeCroy LRS 234L Linear Amplifier, serial no. 9007, datasheet found at `http://www-esd.fnal.gov/esd/catalog/main/lcrynim/234-spec.htm`

[12]HV4032A7P and HV4032A7N respectively

pod supplied up to -3kV[13]. We used the ± 7kV pods to charge the RPC resistive electrodes and the -3kV pod to supply the photomultiplier tubes on the scintillating paddles (see section 5.11).

The LeCroy unit supplied a maximum current of 2.5mA via the -3kV pod and a maximum current of 500μA through the ± 7kV pods.

5.3.1 Safety interlock

The unit featured an interlock which would only supply the high voltage if +5V was delivered to the interlock terminal through a BNC connector. We developed a simple, mains powered unit which was switched on when the fume cupboard door was shut thus preventing us from coming into contact with our RPC whilst it was live. The unit featured a red warning led which alerted you when it was switched on.

5.4 Resistive electrode coating

Finding a suitable resistive coating proved to be difficult. Glass proved difficult to apply any fluid to evenly without puddling and many of the coatings we tried were too resistive.

We knew that we were aiming for a surface resistivity of at least $10^5\Omega$/square[20] so that signals would be well localised. To test surface resistivities small samples of the glass to be used in the RPC[14] measuring approximately 100×100mm were coated in a square shape and two lines of silver paint were applied to two opposite sides of the square. A voltage of 30.5V was put across the square and the current measured in an ammeter sensitive up to 0.01μA. This effectively placed a limit on our setup of $3.05 \times 10^9\Omega$/square.

In hindsight it may have been better to use the four point probe technique which eliminates any voltage drop due to imperfect electrode contact[21].

Assuming unit thickness, the surface resitivity of the coating ρ is given by,

$$\rho = Rw/l$$

where R is the resistance of the sample, w is the width and l is the length. Since the samples are squares $w/l = 1$ and so $\rho = R$.

5.4.1 Preliminary tests

The first samples were painted on with a brush and there was large differences between repeat experiments. It was decided that the variation was due to uneven application over a relatively small square size (generally about

[13] HV4032A1N

[14] Standard 2mm Pilkington's float glass – See J. Rowden in glass workshop for data sheet

50mm^2). We overcame this problem to a certain degree by using a spray gun, however if too much was applied then puddling still happened.

Indian inks We were advised by our supervisor that indian ink was often used, the graphite providing the conducting portion of the blend. we tried several brands with the following results,

- *Winsor Newton* – Resistivity beyond the range of setup ($> 10^9\Omega$/square)
- *Ocaldo* – Initial tests showed some measurable resistivity, however subsequent tests proved that this was due to uneven application. Spray application required up to seven coats before resitivity could be measured which became impractical considering that subsequent coats resulted in blistering of existing coats unless great care was taken.
- *Schwartz* – Resistivity beyond range of setup.
- *Unbranded ink sample* – resistivity beyond range of setup.
- *Dr. Martin's Bombay* – The Bombay ink proved to be the best candidate. Typical single coats resulted in initial resistivities of around $30k\Omega$/square.

we continued the investigation using the Bombay brand.

Other coatings Other coating were trialled, an unlabelled bottle of graphite paint found in the laboratory proved to be too resistive to measure, the Aquadag/Electrdag range of graphite paints were all too conductive[15], John Rowden in the glass workshop suggested applying photocopier toner and then baking it into a hard resin, which we did by mixing with ethanol and spraying, however this too proved too resistive.

We found some antistatic spray at RS[16] with suitable resistivity properties ($10^7\Omega$/square) although it was meant for acrylic not glass and our budget did not allow us to experiment.

5.4.2 Tinned versus non-tinned sides of glass

Due to manufacturing techniques in flat glass, one side is invariably contaminated with tin which reduces the resistivity by up to a factor of 100. This can be determined by shining ultra-violet light onto the glass, the side that 'glows' is the tinned side.

Since the Bombay ink tended to be slightly too conductive, we coated our second and third prototypes on the non-tinned side. Comparisons of tinned versus non-tinned can be seen in the results for varying the sample sizes.

[15] See `http://www.achesonindustries.com/`

[16] RS no. 247-4273

5.4.3 Drying times of inks

As the inks dried the resistivities changed. To measure this a long-term drying experiment was initiated to study how long inks took to dry and what effects they had. From preliminary tests we suspected that baking the samples made them more stable. Because of this we performed the test on six samples each having undergone three different heat treatments as listed in the table below. Each of the conditions were doubled up to get an average.

Sample number	Treatment
1,2	None
3,4	Baked at 70°C until dry
5,6	Baked at 200°C for 15minutes

The samples were left in the laboratory exposed to the air over a number of weeks. The results are shown in figures 19 and 20.

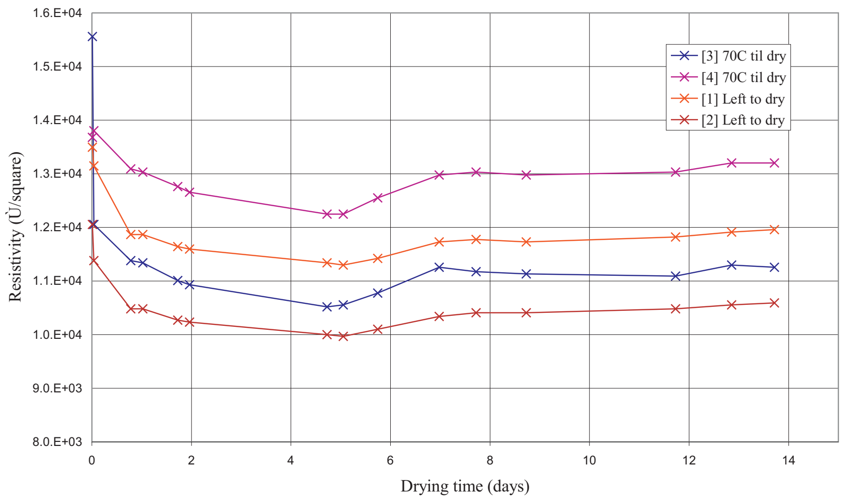

Figure 19: Effects of long term drying over a period of 14 days

The resistivity of all samples initially decreased before rising again and settling after seven days. Later results taken four weeks later showed that the resistivities had not changed significantly since then. It is also interesting to note that the samples baked in the oven at 200°C were much more stable. they did not vary so greatly as the others and settled sooner than the other after only one day.

In order to have consistent resistive properties in our coating, we should bake our samples at 200°C for fifteen minutes.

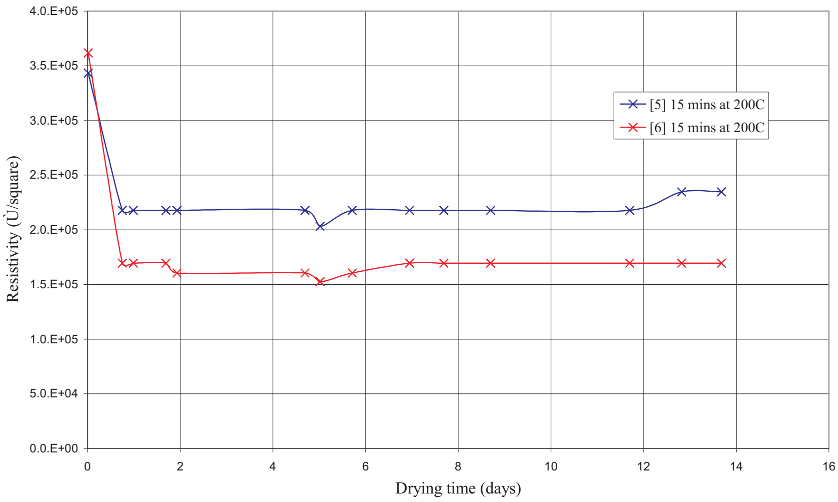

Figure 20: Effects of long term drying over a period of 15 days for the samples baked at 200° for 15 minutes

5.4.4 Varying sample sizes

One rather surprising observation in the preliminary tests was that larger square sizes consistently resulted in higher resistivities. An example was the Bombay ink sample of square size 78mm^2 which was half as conductive as a Bombay sample of 50mm^2. This implies non-ohmic behaviour in the inks which should be investigated.

To test this we used two samples of glass measuring 200×180mm and covered one side completely, one of them had the tinned side coated, the other was sprayed on the non-tinned side. Two polished aluminium strips were placed onto the ink surface so as to form a square, the current was measured passing through the sample at 30.5V. To reduce the square size, ink was scraped off using a Stanley blade and a steel ruler.

In all our trials the samples were baked for fifteen minutes at 200°C. For the first trial the samples we the tests commenced twenty minutes later which means that there still could have been drying taking place. To compensate for this the same samples, after testing were resprayed and baked again and resistivities were taken after twenty minutes for the same duration as the initial experiment without adjusting the sizes. The results are shown in figures 21 and 22.

For the second trial, to make sure drying was not influencing our results, we baked the samples in an oven at 200°C for fifteen minutes and left the samples for four days before scraping took place. The results for this trial are shown in figure 23. The results in figure 22 show very little change,

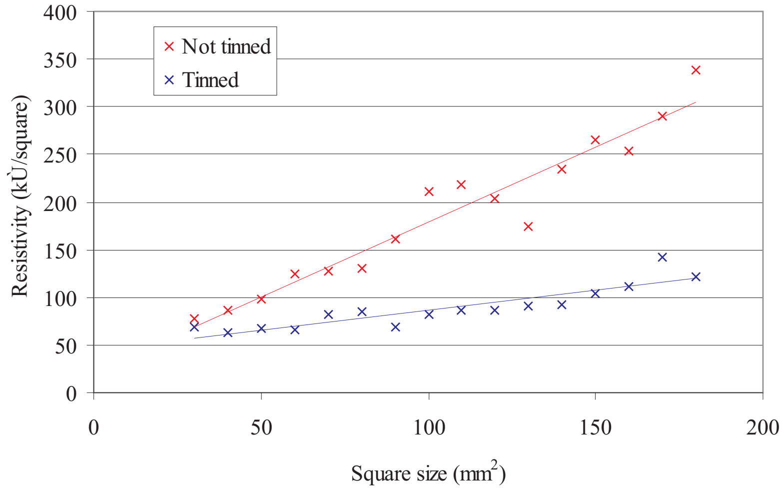

Figure 21: Adjusting the square size after twenty minutes drying

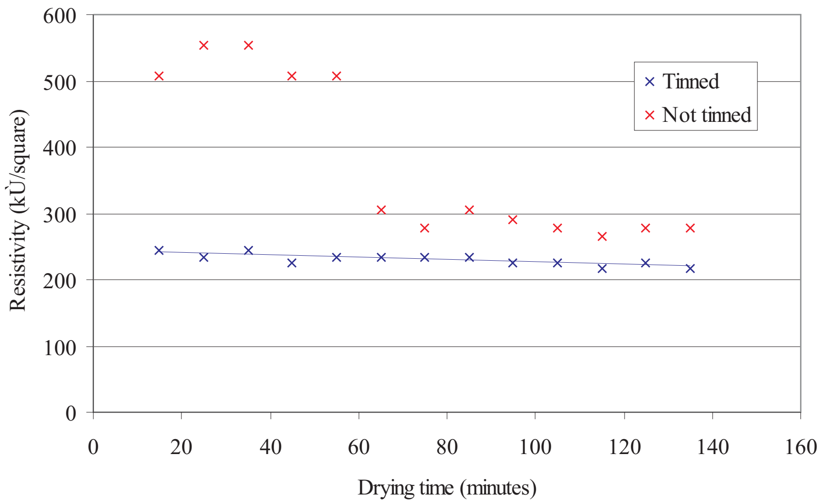

Figure 22: Compensation for drying for the duration of the square size trials. Note that the jump in results for tinned is almost certainly due to a surface contaminent which was removed halfway through the trials and so was ignored

certainly not enough to affect the figures in the square size test, even proportionally. This suggests that the square size figures are largely unaffected

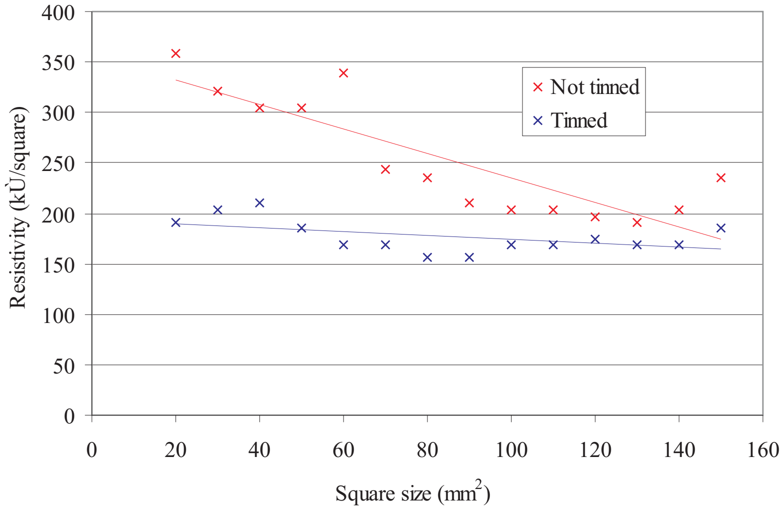

Figure 23: Adjusting the square size after four days for drying to stabilise

by drying. It is interesting then to note that the square size does affect the resistivity properties of the samples in a linear fashion indicating non-ohmic properties, the larger the square the more resistive it is. The second trial which performed the same tests but after four days of drying also shows a relationship but it is much less pronounced, in fact it could be interpreted as being inclined the other way, the larger the square the less resistive it is. Since the test was repeated only twice the standard deviation does not provide a clear verification of this. It appears that the non-ohmic variation of resistivity with square size decreases with time, perhaps because it is related to the water in the ink which disappears as it dries.

5.5 First prototype

All the prototypes followed the same basic geometry shown in figure 24 In reference to figure 24, the first prototype dubbed 'Jerry-Beth' was of the following dimensions,

Dimension	Size (mm)
w_{int}	250
l_{int}	250
w_{ext}	315
l_{ext}	300
w_{elec}	225
l_{elec}	195

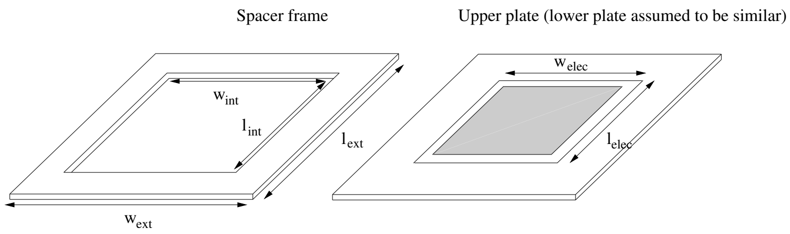

Figure 24: Geometry of the prototypes, electrode dimensions taken from outside of copper tape which is 10mm wide

The dimensions are fairly typical of prototype RPCs used for investigations. Jerry-Beth was coated with ink before the investigations into resistive properties were completed and as a result was assembled with the tinning on the outside of the chamber. In addition, when selecting the epoxy to use we were primarily concerned with it being a slow drying one, five minute epoxy would begin to dry as soon as it was applied and applying the fragile glass frame to a layer of epoxy which has dried unevenly could cause it to break. Unfortunately standard epoxy has poor chemical, electrical and heating properties. Placing the detector in the oven to dry, even at 70°C caused the epoxy to go tacky. Moreover we spread the glue onto the glass and mixed it there resulting in much more epoxy than was needed. Much of the epoxy spilled over the side and into the chamber.

We chose not to experiment with Jerry-Beth due to uncertainties in the electrical properties of the epoxy and unsuitable resistivity characteristics.

5.6 Second prototype

Our second prototype dubbed 'John-Lauren' was of the dimensions in the table below.

Dimension	Size (mm)
w_{int}	245
l_{int}	245
w_{ext}	280
l_{ext}	280
w_{elec}	180
l_{elec}	175

In our second prototype we used 2014 Araldite[17] along with disposable mixer-applicator. This time there was no overspill around the edges which may have provided a conducting path for the HV. We applied a coat of Bombay ink onto the outside (non-tinned) side and baked the chamber for

[17]RS no. 332-1748, datasheet available on RS website

15 minutes at 200°C. The final surface resistivites of the resistive coatings were $3.05 \times 10^5\Omega$/square on the topside and $2.54 \times 10^5\Omega$/square.

The whole unit was held together by two plywood panels bolted at the edges. These rested over the top of the readout plates bridging both the actively used readout plate and earth. In hindsight this was probably not a good a idea considering the bulk resistivity of wood can be as low as 10^2–$10^5\Omega$.cm[18] which probably damped the readings. For the final design we envisage fixing the readout unit permanently onto the chamber thus not needing the clamp.

All our trials were done with this prototype.

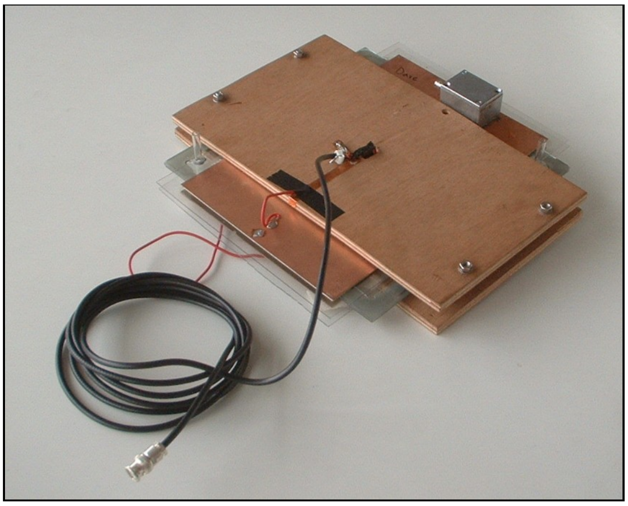

Figure 25: The fully assembled RPC unit

5.7 Third prototype

The ill-fated third prototype, dubbed 'Richard-Laura' has the dimensions listed in the table below.

Dimension	Size (mm)
w_{int}	250
l_{int}	250
w_{ext}	300
l_{ext}	300
w_{elec}	183
l_{elec}	183

The third prototype was to be an investigation into different gap widths, research has suggested that a gap with below 1mm inhibits streamer growth

[18]For distilled wood[31]

by around a third[30] which may reduce the need for quenchers. In addition a narrow gap would mean that a lower voltage would need to be applied in order to generate the same electric field which could bring it within the CLEAPSS regulations.

One of the few materials we found that was available in sheets less than 2mm thick was PETG Copolyester[19]. The dielectric strength was suitably high at 16kV/mm.

Unfortunately we assembled the RPC before the ink investigations were fully completed and so before we knew that it would be necessary to bake the ink to make it stable. We were aware that the coefficients of linear expansion differed by a factor of 10 before we placed it in the oven at 200°C although we already had a working prototype at this point and so we decided to chance it. When we removed the plate it was still in tact until we placed it on the bench to cool, the impact caused a large crack to appear on the upper plate. We later tested it to see if it leaked argon, which it did. We therefore decided not to use this chamber. Ironically, if we had used the plain Araldite epoxy which turns tacky as it heats up, the chamber may have remained intact!

5.8 Electrically reinforcing the design

Initially the readout system would spark under voltages of around 1kV causing the HV unit to trip out. We isolated each component and tested it separately. We replaced the wire taking the HV from the SHV socket to the PCB inside the aluminium box with a shorter, stiffer length that would not rest against any of the walls of the box, we also removed more of the copper around the hole where the tape wrapped around onto the bottom of the PCB and sprayed the inside of the box with insulating PCB lacquer. We tested this and generally it held at the maximum 7kV the supply output, it tended to breakdown just under the maximum when both plates were assembled together presumably due to the combined fields.

We discovered that the fibreglass substrate on the PCB in the readout system broke down under around 3kV of potential. We reinforced this with a layer of the same copolyester used in our third prototype which has a dielectric strength of 16kV/mm. This is less than optimal however since the readout strips are now 3.6mm away from the resistive electrode resulting in weaker induced signals. In future designs we believe that it would be better to make the readout strips out of a sheet of 1mm copolyester and strips of copper tape and not to bother with the PCB.

Once these problems had been ironed out, the chamber broke down at $\pm 3.5kV$ (7kV in total) when fully assembled when filled with air. Adding a gas mixture of argon, freon and butane in a 40/50/10 mix we could take

[19] RS no. 334-6444, see RS website for datasheet

the chamber up to ±6kV reinforcing the notion that we need quenchers to prevent all-out discharge in high electric fields.

5.9 Gas mixtures used

Although we planned on testing a freonless gas, the alternatives tended to use oxygen. Since we did not want to experiment with such a reactive gas at this early stage in the interests of safety we decided instead to try some more traditional mixtures of argon, freon and butane. We used existing mixes as our starting point, the Belle experiment at the Kek facility uses a mixture in the proportion 30/62/8[20]. We initially decided to try a more conservative mix of 40/50/10 since we were aiming for as little freon use as possible.

5.10 Electrical resonance

Figure 26 shows a typical cosmic ray signal from the RPC at ±5kV with the 40/50/10 gas mix before amplification. We see a definite oscillatory

Figure 26: Cosmic ray signal in coincidence with the scintillators (upper trace), time base 100nS per division, RPC trace set at 2mV per division

behaviour with a period of 10 nanoseconds. We considered initially that it could be due to ripples in the high voltage supply, since the LeCroy manual warns about this on the second page, however this resonant behaviour was present even when the RPC was disconnected from the HV supply, figure 27 shows this. In fact a peak-to-peak signal of up to 10mV built up over a period of about 10 seconds which was very difficult to stop, even after disconnecting the BNC cable from the readout unit the resonance continued. We presume this was driven by Johnson noise since it occurs initially without any voltage applied[32]

[20]In fact silver butane (70% butane, 30% iso-butane) is used in place of butane at the BELLE experiment

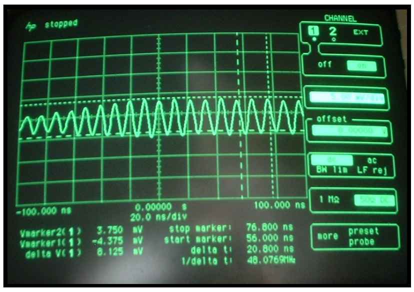

Figure 27: Resonance without the HV supply connected, time base 20nS per division, signal scale 2mV per division

Resonance occurs in electrical circuit that features an inductance and a capacitance. Although our circuit includes neither an actual capacitor nor inductor components, there are 'ghost' capacitances and inductances which are unavoidable features of actual circuits, for example the co-axial cable has a capacitance since we have two electrodes separated from each other by a small distance, current flowing through even straight wires causes at least a little inductance. There are two types of resonant circuit, series and parallel, figure 28 illustrates them both. Possible candidates for the

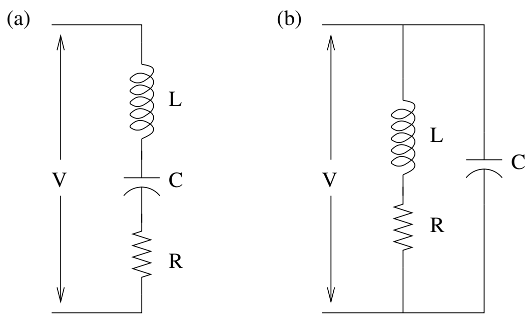

Figure 28: The two resonant circuits, (a) is series, (b) is parallel

capacitance in our circuit are the plates themselves and the capacitances of the coaxial cable. Using the formula $C = A\epsilon_0\epsilon_d/d$ and assuming that the dielectric constant (ϵ_r) of the PETG and the phenolic resin and paper substrate is 2.4[31] and 5–6[33] respectively, and the two layers make up two capacitors in series, then the capacitance is 566nF. According to the datasheet the coaxial cable (URM43) has a capacitance of 100pF per metre. Likely candidates for the inductance are the BNC cable and the wire soldered to the readout plate.

The resonance continued even after the readout unit was discontinued just in the BNC cable alone at the same frequency. This implies that the capacitance causing the 10 nanosecond period resonance is due to the BNC cable. The cable was 3 metres long with 100pF per metre giving a total capacitance of 300pF. Assuming that the BNC cable on its own is a resonant series circuit which obeys the formula $\omega = \sqrt{1/LC}$[34], we can then calculate the inductance in the cable ($\omega = 2\pi \times 10^{-8}$). The inductance of the BNC cable works out at, $8 \times 10^{-}9$H.

When the BNC cable is detached larger, less frequent oscillations die down. This implies that there is more resonant frequencies probably due to the capacitance in the readout strips. Ideally we could study this with a frequency analysis on the oscilloscope however our oscilloscope did not have the facility for this.

We attempted to damp the resonance using a resistor inserted into the readout circuit using a BNC cable with crocodile clips. Unfortunately this made no difference. It seems that the noise which appears to be causing the resonance 'triggers' the resonance too often for this to be effective. We attempted to change the frequency of the resonance by inserting capacitors of both 220pF and 2200μF in series with the circuit although this made no difference to the signal. We also tried an inductor in series but this too did not affect the frequency of resonance noticeably.

In the end we decided to continue with the efficiency tests regardless of the resonance, the peak-to-peak voltage pulse shape was approximately that of a capacitor discharge and so if the threshold was set high enough and the pulse duration long enough it would bridge the resonance oscillations.

5.11 Method for determining efficiency

Efficiency can be defined as follows,

$$\text{Efficiency} = \frac{\text{Particles detected}}{\text{Particles passing through detector}}$$

In order to determine the amount of particles that pass through our detector we sandwich our RPC between two scintillator detectors, denoted A and B. If A and B both detect a particle then we can assume that it passed through our chamber[21] Each time this happens we count whether or not the RPC registered a 'hit' and if it did this counted towards the tally of 'particles detected'.

In order to do this we used the following electronic arrangement, The discriminator unit outputs a digital pulse if the input exceeds a set threshold voltage, all three detector signals were digitised in this way. The pulses from this unit are then delivered to the coincidence unit which behaves like an AND gate. If a pulse from A and a pulse from B coincide in time then the

[21] In practice this turned out to not be the case due to the geometry of the setup, see section 5.11.2.

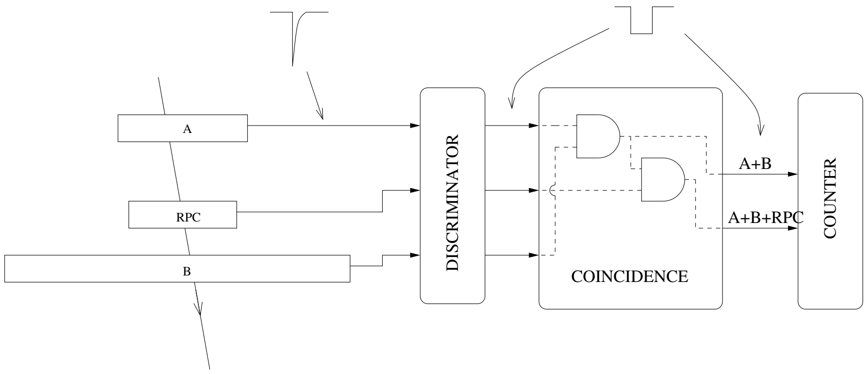

Figure 29: Processing detector signals for determining efficiency

first AND gate outputs a pulse. A second AND gate was configured whose inputs were the output from the first AND gate and the discriminated RPC signal. The two outputs from the two gates were counted in the counter unit, effectively counting the coincidences of the two scintillators and the coincidence of all three detectors. The discriminator could only discriminate above 50mV and so the RPC signal was passed through a 10 fold linear amplifier[22]. The duration of the voltage pulse output by the discriminators depended on a length of BNC cable which was connected. The scintillators after the AND gate generally output a coincidence pulse of around 60nS, the RPC discriminator signal was generally 10nS long.

In practice the scintillators were not 100% efficient, approximate guesses were around 40% based on an expected cosmic ray flux of 1 every 10cm^2 a second. Provided that the particles detected were a random cross section of cosmic rays this should not be a problem, however it is more likely that particles of a certain type were less likely to be detected (possibly lower energy electrons or muons). As a result we can only make guesses for efficiency for the types of particles that were detected by the scintillators.

5.11.1 Scintillator detectors

The scintillating detectors were two blocks of solid scintillator with the light guides and the photomultiplier tube built into one unit. The upper scintillator was formed into a paddle and had approximate effective detection dimensions of $110 \times 100 \times 5$mm and required a supply of 1.86kV to function. The larger, lower block of scintillator was encased in a wooden box with an estimated effective area of $600 \times 300 \times 70$mm (in both case the effective areas could only be estimated at since they were enclosed). Both scintillator units were wrapped in bin-liners in order to keep out any photons from ambient

[22]LeCroy LRS 234L serial no. 9007

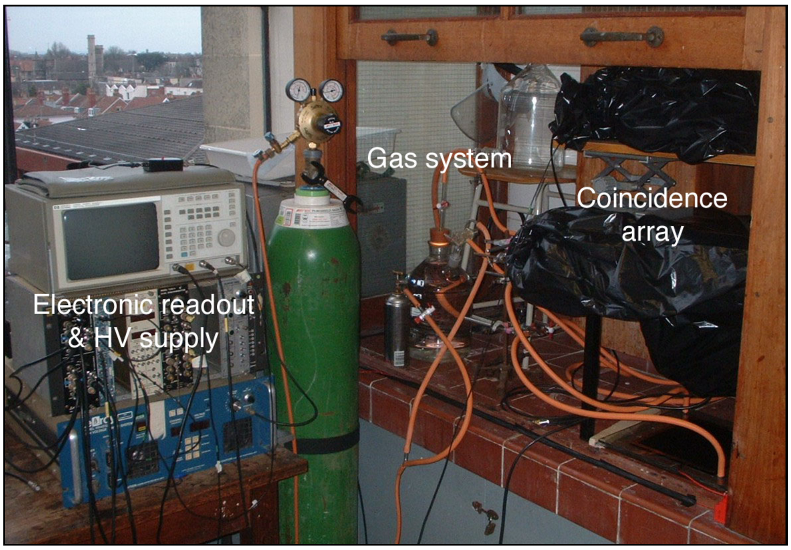

Figure 30: Full experimental setup. Note that the RPC would normally sit between the two scintillators in the coincidence array

light which may cause false trigger in the photomultiplier tubes.

5.11.2 Coincidence modelling

We were restricted in what scintillator detectors we could use and had to use a less than optimal setup. The scintillators were not immediately above and below the RPC and the bottom scintillator was much larger than the RPC meaning that particles could pass through both scintillators without entering the RPC. In order to compensate for this a Monte-Carlo model was formulated which modelled this arrangement. It generated cosmic ray particles with typical velocity vectors, in particular the $\alpha \cos^2$ distribution, and passed it through the modelled array, registering which detectors it passed. it output the percentage of times we could expect the RPC to register a hit when a particle passed through both scintillators.

We ran the program several times since it was a Monte-Carlo style simulation and so statistical in nature. Assuming the effective volume for our detector was as deep as the gas gap and covered an area the size of the read-out plate, we get can expect $20 \pm 1\%$ of the particles which pass through the scintillators to pass through our detector. As a result, we should multiply our counts for the detector by five in order to correct for this. However signals could also be picked up on the readout strips that occur further out on the HV electrodes, as a result we also calculated for an effective area the size of the HV electrodes which gives $55.8 \pm 1\%$ for John-Lauren. Both of these corrections were plotted in the results giving a range of efficiencies.

More about the model and other models can be found in appendix D.

5.12 Noise

The signals that we were observing as cosmic rays typically had a maximum peak-to-peak size of around 30mV amongst a reasonably constant resonant noise level of just under 10mV. This corresponds to a noise level of 9.5dB (using $20\log_{10}(V_{signal}/V_{noise})$.

5.12.1 Fitting noise to the data

In preliminary tests the count rate of the RPC after discrimination was haphazard. Sometimes jostling the wires caused an enormous jump in the count such that the nine digit counter was not enough. In order to verify that the signal coincidence were not merely due to random noise a program was written to determine how much random noise was needed in order to generate the coincidences, this was then compared to actual signal counts to see if they matched up.

The calculations assumed a coincidence signal of 60nS in length every 1.5 seconds and noise signals of 10nS in length. If $P_n(h)$ is the probability that the n^{th} noise signal hit and $P_n(m)$ is the probability that the n^{th} noise signal misses then the model calculates the number of noise signals to generate a certain coincidence ratio by the following process.

Number of noise signals	Probability of a coincidence
1	$P_1(h)$
2	$P_1(h) + P_1(m) \times P_2(h)$
3	$P_1(h) + P_1(m) \times P_2(h) + P_1(m) \times P_2(m) \times P_3(h)$
	etc.

The following values were used for the probabilities,

$$P_n(h) = \frac{f_{\text{signal}}}{n\Delta t_{\text{noise}} + \Delta t_{\text{signal}}} \quad (1)$$

$$P_n(m) = 1 - \frac{f_{\text{signal}}}{n\Delta t_{\text{noise}} + \Delta t_{\text{signal}}} \quad (2)$$

The following assumptions are made:

1. Only single coincidences occur
2. The noise signals are spaced far apart in comparison to their duration (this means that we can ignore spaces between two close noise signals which are less than 10nS in size and so unable to accommodate a noise signal)

The probability calculations were written up in a Python script which incremented the number of noise signals until the probability reached the ratio of triple to double coincidences.

The code can be found in Appendix D.4

5.13 Electron versus ion signals

The results which showed cosmic rays were taken with the negative electrode at the top. At one point we ceased to get any pulse coinciding with the scintillators from our detector and we believe that it is because the electrodes were swapped. Unfortunately we discovered this too late to perform any more tests and will have to be resolved by next years project students.

There is evidence that reversing the polarity and therefore the type of discharge picked up in the readout system would be different for electrons and ions, certainly in term of timing, electrons have a much higher mobility than ions, but also in terms of amplitude of signal (see texts on multiwire proportional chambers).

6 Results

Figures 31, 32 and 33 show the corrected coincidence rates for the RPC at different voltages. Figures 34 and 35 show results for a trial undertaken with the same gas mixture which had been sat in the chamber over the weekend and with it replenished respectively to give some idea of how the chamber behaved over time. The error is the standard deviation of four trials apart from the results testing for age tests which were done over three trials. All trials were done using a gas mixture of 50% argon, 40% freon and 10% butane. The curves are fit to data. Figure 36 shows the necessary

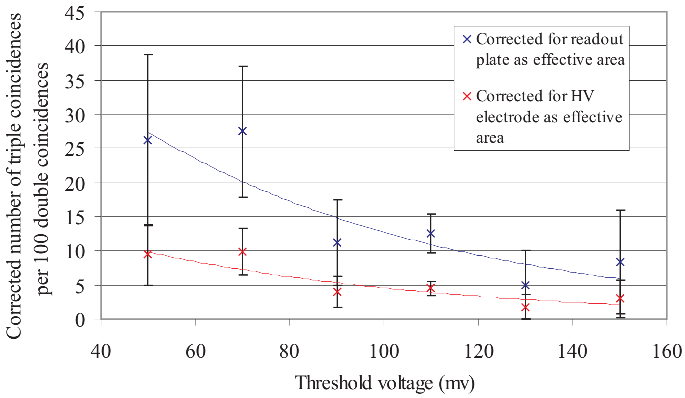

Figure 31: Number of triple coincidences at ±4kV for every 100 double coincidences versus threshold voltage

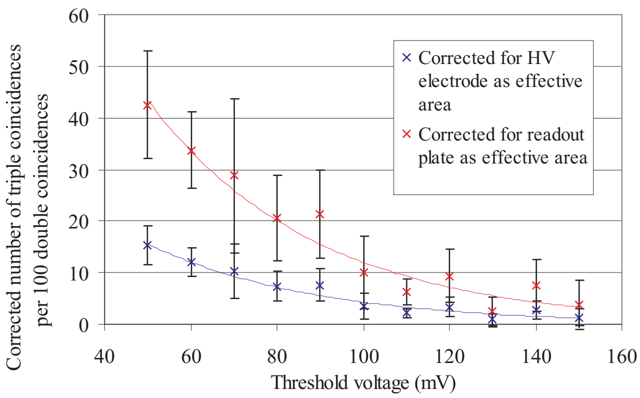

Figure 32: Number of triple coincidences at ±5kV for every 100 double coincidences versus threshold voltage

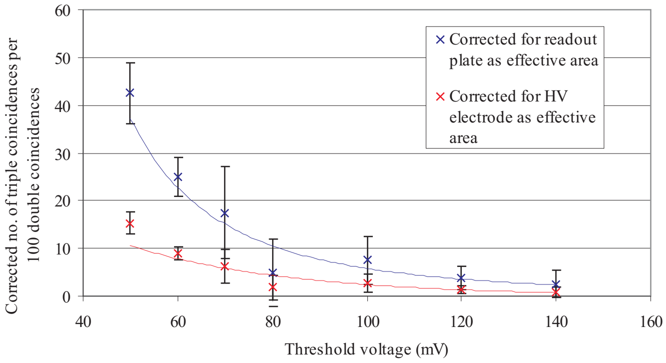

Figure 33: Number of triple coincidences at ±5.5kV for every 100 double coincidences versus threshold voltage

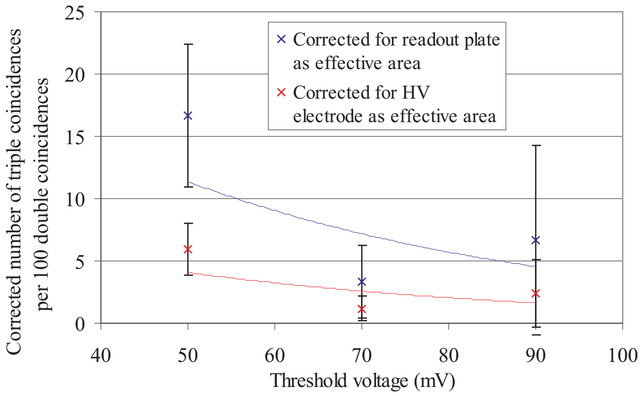

Figure 34: Number of triple coincidences at ±5kV for every 100 double coincidences versus threshold voltage. Taken with the gas mixture having been in chamber over the weekend

random noise counts needed to generate the signal observed versus the actual counts taken from an RPC reading. The error in the random noise needed was calculated by adding and subtracting one standard deviation from the inputs. There was no error available for the count rates since only one trial was undertaken.

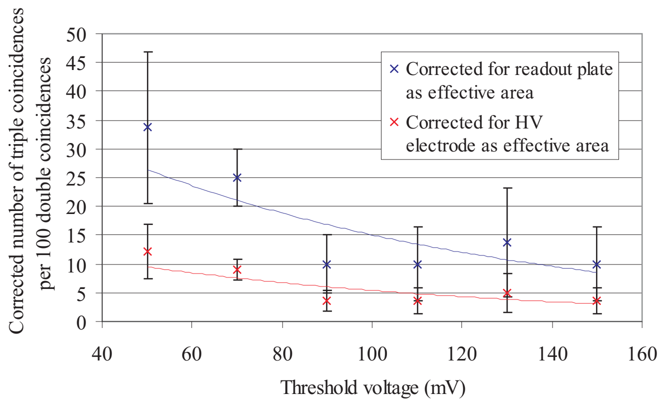

Figure 35: Number of triple coincidences at ±5kV for every 100 double coincidences versus threshold voltage. Gas replenished after previous trial

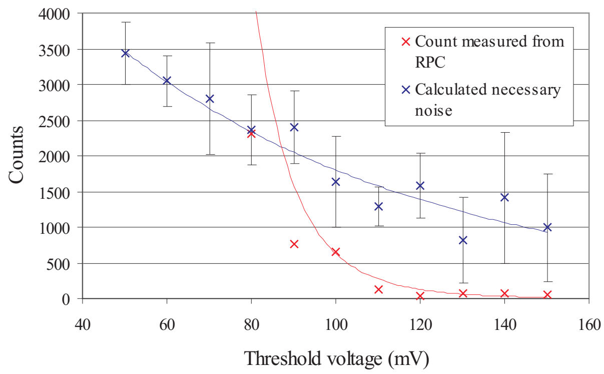

Figure 36: Measured RPC count rate for ±5kV and calculated random noise needed to replicate results versus threshold voltage

7 Discussion

7.1 Noise from the RPC

We see in figure 36 that the point where the signal count crosses the noise count is at around 90mV. For thresholds below this, the coincidences are almost certainly due, at least in some part, to noise. Above this threshold the coincidences are at least partially due to the RPC.

There is a discrepancy however in that the RPC was outputting a huge number of counts yet the coincidence rate does not go up accordingly, for a random noise level that high, one would expect an almost certain coincidence probability. It should be stated that it was not possible with our setup to count both the number of times the RPC output a signal, the number of scintillator and triple coincidences since we only had two counters, the results we see on the graph were from two different trials under the same conditions and so in practice these may not be consistent. Ideally we could have taken an average over several trials of RPC counts (the triple coincidences were already averaged over four trials) however time did not permit this. The second explanation for this disparity is that the noise from the RPC was not random in nature. The huge counts could have originated from occasional periods of high noise activity, such as from jostling a wire. this aside, the results here suggest that we should ignore any efficiency reading for threshold below 90mV.

7.2 Efficiencies

Since we do not know for sure the exact size of the effective are of the RPC which affects the correction factor, it is only possible to give a range of value for the efficiencies of the RPC at different voltages. The ranges also take into account the gradient above the 90mV threshold. These are tabulated below.

Voltage (kV)	Range of efficiencies
±4	2%–15%
±5 (averaged over two trials)	2%–16%
±5.5	1%–7%
±5 (left over weekend)	2%–4%

Although there is a difference in efficiencies they appear to be minimal. Aside from the ±5kV trial, these results are based on only one trial each and so it is difficult to say if the difference in efficiency is significant. However, leaving the gas over the weekend certainly seems to have adversely affected the efficiency. This could be due to a slow leak in our gas system which was undetectable using soap bubbles, or perhaps it is due the some kind of settling of the gases, again it is difficult to draw conclusions without further tests. The efficiency, although low could no doubt be improved upon by refining the gas mixture and honing the voltage to it optimum.

7.3 Cost estimate

The following is a breakdown of costs for theoretical new RPC incorporating all the recommendations made in this report such as 1mm copolyester gas gap and improved readout strips made from copolyester and copper tape.

Material	Cost per unit (£)	Used for	Cost (£)
RPC Unit			
Pilkingtons float glass	36.00 per sheet	2×resistive plates	6.00
Araldite 2014 epoxy	8.40 per 50ml	∼ 1/4 tube	1.10
PETG Copolyester	8.57 per sheet	spacer frame and readout [23]	1.07
Conductive copper tape	32.48 per reel	electrodes and readout	1.97
SHV sockets	5.20 ea.	2× for HV plates	10.40
SHV connectors	13.04 ea.	4× for two HV cables	52.16
URM43 coaxial cable	25.62 per 100m	∼ 9m for readout and HV[24]	2.30
Aluminium enclosure	2.07 per box	2× for HV and shielding	4.14
Bombay ink	2.40 per jar	∼ 1/4 jar	0.60
		Total	79.74

HV power supply cost depends on what the optimum voltage is. Presuming 5kV is our maximum, Spellman HV's 'MM' units[25] cost £47. The SHV connectors increase the cost dramatically. If a custom HV supply which was mounted directly on the RPC could be formulated then this would save over £60. It is also possible to make your own HV supply from simple electronics[23] however, this may be too risky for classroom use.

Readout system cost depends on what kind of electronics is desired. Presuming simple counter style electronics as shown in appendix C then cost of electronics would be less than £10. Progressing onto data logging on a PC via serial interfaces would mean an expensive PCI card (∼£200–£300), also since we had a request for compatibility with Mac computers which generally do not have serial ports this would mean even more expensive USB interfaces[26]. Project work for next year could be designing and building a less expensive USB interface as well as a cross platform software API for this.

As for collaborative arrays, the problem with keeping the units in precise synchronised time has been resolved in the past by using GPS units at each station. This inflates the cost greatly, the electronics for the SEASA project was costed at 6500 SEK (about £480). However this was done in 2002 when GPS was still a relatively new technology, a similar setup today would undoubtedly cost less.

The final cost for the unit depends a great deal on the electronics and power supply used since the materials used in the actual RPC (minus SHV cables) cost less than £12. A minimal unit with simple counter electronics and an onboard custom power supply of, say, £50 could be driven as low as £75.

[24]both can be cut from same square of plastic

[24]Assuming final design does not surpass ±5kV operating voltage

[25]Product spec. found at http://www.spellmanhv.com/pdf/MM.pdf

[26]Adept Scientific sell USB units for around £450–£600

8 Conclusions and Further Work

The RPC detector shows great promise although we are still a long way from a final product. We have demonstrated that the RPC does detect cosmic rays in coincidence with the scintillator array albeit at a much lower efficiency. Work needs to be done in refining the gas mixture as well as fining the optimum voltage, ideally the gas system could be tweaked so that it would be suitable to take oxygen and so the freonless, non-flammable mixtures can be tested[5].

The third prototype could be re-created (this time with the ink coating applied and baked *before* assembly) and investigations into 1mm gap design could be undertaken since the narrow gap makes it almost self quenching[30].

Readout electronics could be developed and computer interfacing could be looked into. The diagram in the appendix provides a good starting point. The final design may have several readout channels corresponding to several strips and so the logging software would have to deal with this.

Making the RPC visual is also of importance for teachers. This would suggest a streamer mode detector which was entirely transparent using resistive electrodes other than ink. Research into photographing streamers could be useful for this[28].

There is obviously plenty of scope for further investigation into RPCs, although during our investigation we came across a number of other detector designs which may or may not be suitable for this project. An enthusiast at `http://www.cosmicrays.org/` has successfully designed and built a multiwire proportional chamber using amongst other thing an old refrigerator pump to create a low pressure environment. The BNL laboratories developed a detector which used Ĉerenkov light using a Thermos flask and a photomultiplier tube. Full instructions were available until recently online and may still be available on request[27].

[27] Try contacting the via `http://cosmicray.bnl.gov/contacts.html` in reference to 'Thermos Bottle Detector'

A Survey of physics in secondary schools

A survey was placed online[28] and advertised on the Institute Of Physics PTNC (Teachers) mailing list, Times Educational Supplement forums and a mailing list of local physics teachers. In all we got 35 responses (in fact we got 36 but one was from a Canadian schoolteacher and so was not included in the final results).

A.1 Survey outline

```
Questionnaire for schools teaching particle physics

I am an undergraduate at Bristol University developing an affordable
particle detector for schools. This questionnaire will hopefully give a
better insight into what schools want from a project such as ours.

Specific information collected will not be passed on to commercial
parties, it is purely for our own research.

------------------------------------------------------------------------

Q1.Would you consider purchasing apparatus for the detection of cosmic
rays at a low enough price?

Q2. What would be the maximum you would be willing to spend on such a
piece of apparatus?

Q3. Would you use the equipment primarily for investigation or
demonstration purposes?

Q4.Would your establishment consider collborating with others in the
area to form a 'super detector' similar to the NALTA n the USA?

Q5. It would be a great help if we knew what equipment is already
available to your establishment. Out of the following, which does your
establishment have access to?

    dry ice
    liquid nitrogen
    local source of radiation (i.e. radioactive samples)
    high voltage supply. (Please specify max voltage)
    oscilloscope.  (Please specify: digital, analogue, both)
    a gas trained technician
    laboratory PC
    video camera. (Please specify: digital, analogue, both)
    photographic darkroom
    fume cupboard

Q6. Any further comments or clarifications?
```

[28] http://brendan.sdf-eu.org/misc/detector_survey.php

```
Finally could you enter your name, the name of your establishment and
the level of education which you teach there.

Name:
Establishment:
Level of education (i.e. GCSE, A-Level etc.):
```

A.2 Survey results

Full results available on request (results were taken under privacy agreement)

B Pion and muon decays

The following decays with associated probabilities are decays for pions and muons, both are typical components of an extended air shower. These decays were taken from http://www.cosmicrays.org/muon-rays2.php

μ^-	–	muon	μ^+	–	antimuon
e^-	–	electron	e^+	–	positron (antielectron)
π^-	–	pion	π^+	–	antipion
π^0	–	neutral pion	γ	–	photon
ν_e	–	electron neutrino	$\bar{\mu_e}$	–	antielectron neutrino
ν_μ	–	muon neutrino	$\bar{\nu_\mu}$	–	antimuon neutrino

Particle decay			Probability (percent)
π^+	$\rightarrow$	$\mu^+ + \nu_\mu$	99.98770 ± 0.00004
π^+	$\rightarrow$	$\mu^+ + \nu_\mu + \gamma$	$2.00 \pm 0.25 \times 10^{-4}$
π^+	$\rightarrow$	$e^+ + \nu_e$	$1.23 \pm 0.004 \times 10^{-4}$
π^+	$\rightarrow$	$e^+ + \nu_e + \gamma$	$1.61 \pm 0.23 \times 10^{-7}$
π^+	$\rightarrow$	$e^+ + \nu_e + \pi^0$	$1.025 \pm 0.034 \times 10^{-8}$
π^+	$\rightarrow$	$e^+ + \nu_e + e^+ + e^-$	$3.2 \pm 0.5 \times 10^{-9}$
π^+	$\rightarrow$	$e^+ + \nu_e + \nu + \bar{\nu}$	$< 5 \times 10^{-6}$
π^-	$\rightarrow$	$\mu^- + \bar{\nu_\mu}$	99.98770 ± 0.00004
π^-	$\rightarrow$	$\mu^- + \bar{\nu_\mu} + \gamma$	$2.00 \pm 0.25 \times 10^{-4}$
π^-	$\rightarrow$	$e^- + \bar{\nu_e}$	$1.230 \pm 0.004 \times 10^{-4}$
π^-	$\rightarrow$	$e^- + \bar{\nu_e} + \gamma$	$1.61 \pm 0.23 \times 10^{-7}$
π^-	$\rightarrow$	$e^- + \bar{\nu_e} + \pi^0$	$1.025 \pm 0.034 \times 10^{-8}$
π^-	$\rightarrow$	$e^- + \bar{\nu_e} + e^- + e^+$	$3.2 \pm 0.5 \times 10^{-9}$
π^-	$\rightarrow$	$e^- + \bar{\nu_e} + \bar{\nu} + \nu$	$< 5 \times 10^{-6}$
π^0	$\rightarrow$	$\gamma + \gamma$	98.8
μ^+	$\rightarrow$	$e^+ + \bar{\nu_\mu} + \nu_e$	~ 100
μ^+	$\rightarrow$	$e^+ + \bar{\nu_\mu} + \nu_e + \gamma$	1.4 ± 0.4
μ^+	$\rightarrow$	$e^+ + \bar{\nu_\mu} + \nu_e + e^+ + e^-$	$3.4 \pm 0.4 \times 10^{-5}$
μ^-	$\rightarrow$	$e^- + \nu_\mu + \bar{\nu_e}$	~ 100
μ^-	$\rightarrow$	$e^- + \nu_\mu + \bar{\nu_e} + \gamma$	1.4 ± 0.4
μ^-	$\rightarrow$	$e^- + \nu_\mu + \bar{\nu_e} + e^- + e^+$	$3.4 \pm 0.4 \times 10^{-5}$

C Example readout electronics

Figure C was found at at `http://www.cosmicrays.org/` and although is designed for Geiger Muller tubes, could easily be adapted for our purposes. It also includes a concidence trigger so two chambers could be used to reduce noise or a double gap chamber could be used.

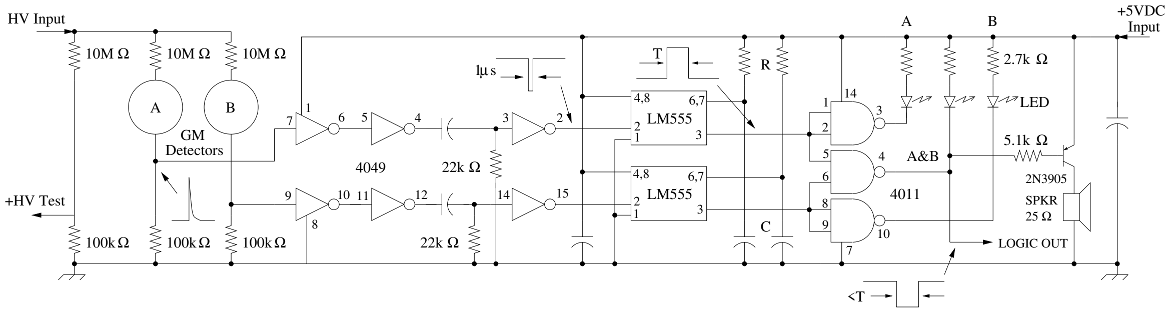

D Computer modelling using python

I chose to use Python[29] to model the detector since it is easy to learn and highly reusable. The module `ParticleModelClasses.py` can be used again by future students to quickly and easily write further models for the detector. There is a brief guide to the module in Appendix D.5

All the computers in the main computer laboratory are currently (2005) equipped with ActiveState's Python interpreter.

D.1 Monte Carlo detector model for determining coincidence rates

```
# coincidence.py
# ---------------------------------------------------------------------
# A Program for determining expected coincidence rates for different
# arrangements of RPC and scintillator paddles

# IMPORT CLASSES

# See separate file ParticleModelClasses.py for classes imported in the
# following statement
from ParticleModelClasses import *

# MODEL VARIABLES

# Takes 'num_sets' number of sets of data. each set has 'events_per_set'
# number of particles run through the model. Take the mean of each set,
# then takes the mean of the set means as the output
num_sets = 30 # Gives generally consistent results
events_per_set = 30

# Define the limits of the model. Should enclose all detectors but also
# be as small as possible to improve speed.
model_limits = Box([600,300,397.5],[0,0,163.75])

# Create the detectors in a list for easy access and expandability
dets = {}
dets['coincidence1'] = Detector([110,100,5],[0,0,360]) # Small paddle
dets['rpc']   = Detector([100,100,2],[0,0,100])        # RPC
dets['coincidence2'] = Detector([600,300,70],[0,0,0])  # Base scintillator

# MAIN ROUTINE

# Creates a particle inside first coincidence detector and passes it
# through the array of detectors logging hits every mm if it is inside a
# detector

# Initiate some vars to store data from each set
ratios = []
```

[29] See http://www.python.org/

```
# Iterate over each set
for set in range(num_sets):
    # Iterate over each particle
    for id in range(events_per_set):
        # Create a particle inside first paddle
        muon = CosmicRay(dets['coincidence1'])
        # Create a place to store all hits from this particle in each
        # detector
        for det in dets.itervalues():
            det.hits[id] = 0
        # Trace particle path through detector group until it leaves
        while model_limits.inside(muon.pos):
            # Check to see if particle is currently inside a detector
            for det in  dets.itervalues():
                # Since detectors tend to be narrow in z direction,
                # check
                # this first to avoid unecessary function calls
                # (improves
                # speed)
                if muon.pos[2] < det.nr[2] and muon.pos[2] > det.far[2]:
                    # Check other co-ords
                    if det.inside(muon.pos):
                        # If particle is inside of detector then
                        # register a hit
                        det.hits[id] = det.hits[id] + 1
            # Update particle position for next iteration
            muon.pos = muon.pos + muon.vel

    # Extract data stored in our detector instances
    rpc_hits = 0
    scrn_captures = 0
    for c1, rpc, c2 in zip(dets['coincidence1'].hits.itervalues(), \
                    dets['rpc'].hits.itervalues(), \
                    dets['coincidence2'].hits.itervalues()):
        if c1 and c2:
            scrn_captures = scrn_captures + 1
            if rpc:
                rpc_hits = rpc_hits + 1

    # Place data for this set in array
    if scrn_captures != 0:
        ratios.append(1.0 * rpc_hits/scrn_captures)


# Print out the data
print 'Calculated from ',num_sets,' sets of ',events_per_set,' ionising cosmic rays:'
print '\t Can expect ', round(100.0* sum(ratios)/len(ratios)) , \
            '% of triggers to have a signal from RPC'
```

D.2 Monte Carlo detector model for determining average path lengths

This is the beginning fo a model to determine the initial ionisation deposited in the detector. At the moment it dertming a distribution of path lengths, eventually it will have a random energy generator according to the distributions given in [13].

```
# path_length.py
# ----------------------------------------------------------------------
# A program which determines typical path lengths for particles in our
# RPC

# IMPORT CLASSES

# See separate file ParticleModelClasses.py for classes imported in the
# following statement
from ParticleModelClasses import *
from dump import *

# MODEL VARIABLES

# Set number of event want to model for the histogram
num_events = 5000

# Set bin increments for histogram (mm)
bin_inc = 0.02

# RPC dimensions x, y, z (mm)
rpc_dims = [180,200,2]

# Reolution of model in mm
resolution = 0.02

# MAIN ROUTINE

# Define model limits so it encloses RPC by least 1 mm on all sides.
# This is because CosmicRay traceback mathod places particle up to 1mm
# inside of model
model_limits = Box([l+2 for l in rpc_dims], [0,0,0])

# Create RPC
rpc = Detector(rpc_dims, [0,0,0])

for id in range(num_events):
    # Create particle
    muon = CosmicRay(model_limits)
    # Create a place to store path length from this particle in RPC
    rpc.hits[id] = 0
    # Trace particle path through model until it leaves
    while model_limits.inside(muon.pos):
        # Check to see if particle is inside RPC
        if rpc.inside(muon.pos):
            # If is inside add 'resolution' mm to path length in RPC
```

```
            rpc.hits[id] = rpc.hits[id] + resolution
        # Update particle posistion for next iteration
        muon.pos = muon.pos + resolution * muon.vel

# PROCESS DATA

# Compiles frequency data for a histogram for use in Excel

# Get lower and upper limits for the histogram
min_val = min(rpc.hits.values())
max_val = max(rpc.hits.values())

# Initialise array to store frequency data
bins = {}
# Not necessary, but makes program easier to read
curr_bin_boundary = min_val
# Iterates over all bins in histogram
while curr_bin_boundary < max_val:
    # Gets a list of values which lie between 'curr_bin_boundary' and
    # 'curr_bin_boundary + bin_inc', then stores the length of this in
    # list
    bins[curr_bin_boundary] = len([x for x in rpc.hits.values() if x >= \
        curr_bin_boundary and x < curr_bin_boundary + bin_inc])
    # Move the bin boundary to the next histogram bin
    curr_bin_boundary = curr_bin_boundary + bin_inc

# OUTPUT

# Outputs a tab separated list of pair values for use in Excel. Use UNIX
# redirect (i.e. 'path_length.py > file.dat') to output to a file.

# Have to use this cludgey code for sorting a dictionary
bin_vals = bins.keys()
bin_vals.sort()
for bin_val in bin_vals:
    print bin_val, '\t', bins[bin_val]
```

D.3 Common detector classes

```
# ParticleModelClasses.py
# ----------------------------------------------------------------------
# Defines the following classes, useful for creating models of particle
# detectors. See each classes docstrign for more information.
#
# Vector    - A list of numbers that behave mathematically as a vector
# Box       - A cuboid in the model, Detector inherits from this
# Detector  - A cuboid detector in the model
# Particle  - A particle with velocity and position variables
# CosmicRay - A particle created in a random position in a space with
#             velocity according to the azimuthal Cos^2 distribution

# IMPORT SOME NECESSARY FUNCTIONS
```

```
from math import *
from random import random

# CLASSES

class Vector(list):
    """Mathematical vector of any size

    Changes behaviour of lists so as to behave more like a vector w.r.t
    addition etc. Methods are described separately. Builds on code by A.
    Pletzer in the ActiveState Python Cookbook"""
    def __add__(self, other):
        "Returns an element by element sum in a Vector"
        return Vector([i+j for i,j in zip(self, other)])
    def __neg__(self):
        "Returns Vector with all elements negatived"
        return Vector([-i for i in self])
    def __sub__(self, other):
        "Returns Vector of the difference of two vectors"
        return Vector([i-j for i, j in zip(self,other)])
    def __mul__(self, other):
        "Returns element by element multiplication in a Vector"
        try: return Vector([i*j for i,j in zip(self,other)])
        # Must be a scalar
        except: return Vector([i*other for i in self])
    def __rmul__(self, other):
        "Since multiplcation commutes, __rmul__() does as __mul__()"
        return self*other
    def __div__(self, other):
        "Divides, element by element"
        try: return Vector([i/j for i,j in zip(self, other)])
        # Must be scalar
        except: return Vector([i/other for i in self])
    def magnitude(self):
        "Returns magnitude of the vector"
        return sqrt(sum([x**2 for x in self]))
    def unit(self):
        "Returns unit vector in direction"
        return Vector(self / self.magnitude)
    def dot(self, other):
        "Returns dot product of this and another vector"
        return sum(self * other)
    def cross(self, other):
        """Returns the cross product of this and another vector.
         Currently only works for Vectors with 3 values"""
        if len(other) != 3 or len(self) != 3:
            raise ValueError, 'cross method currently only works for 3 valued Vectors'
        else:
            return Vector(self[1]*other[2]-self[2]*other[1], \
                    self[0]*other[2]-self[2]*other[0], \
                    self[0]*other[1]-self[1]*other[0])


class Box:
```

```
    """Defines a cuboid in 3D

    First argument when a Box is created is a 3 valued vector giving the
    dimensions of the cuboid, the second argument gives the position of the
    centre. If no arguments given a unit box centred on origin is created"""
    def __init__(self, dims=[1,1,1], pos=[0,0,0]):
        # Note: Do not change the dimensions and position directly,
        # since the corner positions will not be updated and vise
        # versa. Use the 'set' methods below
        self.set_dims_pos(dims,pos)
    def set_corners(self, nr, far):
        "Use to redefine corners of box"
        self.nr = Vector(nr)
        self.far = Vector(far)
        self.dims = Vector([n-f for n,f in zip(nr,far)])
        self.pos = Vector([0.5*d+f for d,f in zip(self.dims,far)])
    def set_dims_pos(self, dims, pos):
        "Use to redefine position and dimensions of box"
        self.dims = Vector(dims)
        self.pos = Vector(pos)
        self.nr = Vector([0.5*d+p for d,p in zip(dims,pos)])
        self.far = Vector([-0.5*d+p for d,p in zip(dims,pos)])
    def inside(self, pnt):
        "Returns True if a point is inside box, False otherwise"
        if pnt[0] > self.nr[0] or pnt[0] < self.far[0]: return False
        if pnt[1] > self.nr[1] or pnt[1] < self.far[1]: return False
        if pnt[2] > self.nr[2] or pnt[2] < self.far[2]: return False
        return True

class Detector(Box):
    """Defines a cuboid shaped detector in 3D

    Inheriting from the Box class, the dimensions and position are
    defined as for a Box."""
    def __init__(self, dims, pos):
        # Run Box constructor
        Box.__init__(self, dims, pos)
        # Define an array to store all particle hits
        self.hits = {}

class Particle:
    """Defines a particle

    Initialises a particle with a position and velocity vector. If no
    arguments given a stationary particle at the origin is created"""
    def __init__(self, pos=[0,0,0], vel=[0,0,0]):
        self.pos = Vector(pos)
        self.vel = Vector(vel)

class CosmicRay(Particle):
    """Defines a cosmic ray particle

     Creates a particle in a cuboid with random direction and
    displacement and traces back to point of entry. Parameter vol is
```

```
    instance of Box or Detector class. If no argument is passed, CosmicRay
    is created at origin"""
    def __init__(self, vol=Box([0,0,0],[0,0,0])):
        # Azimuthal angle according to Cos^2 probability distribution.
        # This uses a Von Neumann acceptance, rejection algorithm, see
        # Section 33.3 Phys. Rev. 2004
        while 1:
            self.phi = random() * pi / 2
            y = random()
            if y <= cos(self.phi)**2: break
        self.theta = random() * 2.0 * pi # Rotational angle of particle
        # Calculate unit velocity vector
        self.vel = Vector([ sin(self.phi) * sin(self.theta), \
                sin(self.phi) * cos(self.theta), \
                -cos(self.phi) ])
        # Place particle in random place in vol
        self.pos = Vector([ random() * vol.dims[0] + vol.far[0], \
                random() * vol.dims[1] + vol.far[1], \
                random() * vol.dims[2] + vol.far[2] ])
        # Traceback the particle position until it is just inside of the
        # vol
        self.traceback(vol)
    # Define traceback function which places particle at entry point to
    # vol
    def traceback(self, vol):
        # Start by skipping 10 mm at a time
        while 1:
            self.pos = self.pos - 10 * self.vel
            if not vol.inside(self.pos): break
        # Place particle back inside detectors vol
        while not vol.inside(self.pos):
            self.pos = self.pos + self.vel
```

D.4 Probability program to predict noise levels

```
# noise_coincidence.py
# ----------------------------------------------------------------------
# A program  for determining how many noise blips are needed to get a
# specified coincidence ratio with a signal of a specified amount.

from random import *
from math import *

# SET VARIABLES

# Signal blip length (S)
sig_dur = 60E-9

# Noise blip duration (S)
noise_dur = 10E-9

# Approx number of signals per second
sig_freq = 1.5
```

```
# Coincidence ratio (ratio between signals:coincidences)
coinc_ratio = input("Enter coincidence ratio: ")

# START MAIN ROUTINE

# We calculate the cumulative probabilities, so we can say 'if we are
# getting 50% coincidences, this could be due to a noise level of N
# blips per second' The maths is as follows,

# P1(cumul) = P1
# P2(cumul) = !P1*P2 + P1
# P3(cumul) = !P1*!P2*P3 + !p1*P2 + P1
# P4(cumul) = !P1*!P2*!P3*P4 + !P1*!P2*P3 + !P1*P2 + P1
# etc.

# Where Pn is the probability of the nth blip coinciding, !Pn is the
# probability of the nth blip NOT coinciding.

# We can use an iterative method (if you look Pn is P(n-1) with an extra
# term) and stop when Pn(cumul) is more than the coincidence ratio.

# ALGORITHM

# Initialise with probability of one blip coinciding
n = 1
Pcumul = (noise_dur+sig_dur)*sig_freq

# We see that the new term in each iteration is comprised of all the !Pn
# from the previous iteration with the extra !P(n-1)*Pn factor. We
# therefore store the series up to !P(n-2) in an array to avoid
# recalculating. This is initialised as 1
Pnot_series = 1

# Keep iterating until we break past the ratio. n will then be set to
# the number we want
while Pcumul < coinc_ratio:
    # Bump up the amount of noise blips 1 at a time
    n = n + 1
    # Calculate !P(n-1)
    Pprev_not = 1 - ((n-1)*noise_dur+sig_dur)*sig_freq
    # Calculate prob of nth particle coinciding
    Pn = (n*noise_dur+sig_dur)*sig_freq
    # Extend array
    Pnot_series = Pnot_series * Pprev_not
    # Calculate current cumulative probability
    Pcumul = Pnot_series * Pn + Pcumul

# OUTPUT

print "Signal blip size: \t", sig_dur
print "Signal frequency: \t", sig_freq
print "Noise blip size:  \t", noise_dur
print "Coincidence ratio:\t", coinc_ratio
```

```
print "Number of noise blips:\t", n
```

D.5 Re-using the detector classes

In order to use the classes in the module `ParticleModelCLasses.py`, you will need to import them into your script. Provided a copy of `ParticleModelClasses.py` is in the same directory as your script the following line should work,

```
from ParticleModelClasses import *
```

After this has been done you now have access to all the objects defined in the file. The first object you will probably want to define is the box which contains your model. To do this you assign it to a variable to create a new instance, along with two lists of numbers, the x,y,z dimensions of the box and the x,y,z co-ordinates of the centre of the model. So for example,

```
model_limits = Box([100,100,100],[0,0,0])
```

After this you will probably want to define a `Detector` in a similar way,

```
rpc = Detector([100,100,5],[0,0,0])
```

Now you can create a `Particle` by specifying x,y,z position co-ordinates and v_x,v_y,v_z velocity components in two lists,

```
electron = Particle([0,0,3],[0,0,-1])
```

This creates a particle just above the 'rpc' with a downwards speed of '1'. To move it we do the following,

```
for t in range(10):
    electron.pos = electron.pos + electron.vel
```

which tracks the electron for 10 seconds along its velocity vector. You will want to include some more interesting code in this loop before it becomes useful.

Python allows you to easily add your own methods and build upon the existing classes using inheritance to suit your needs, for example, say you want to model a particle with spin, you would simply inherit the `Particle` class and add some extra attributes,

```
class ParticleWithSpin(Particle):
    def __init__(self, pos, vel):
        # Initiate as for Particle
        Particle.__init__(pos, vel)
        # Randomly chose up or down (assume random() has been imported)
        if random() > 0.5:
            self.spin = 1
        else:
            self.spin = -1
```

Current attributes cover the needs of the models that I wrote and are documented in the code.

References

[1] An Affordable Particle Detector for Education, M. Saubanère (2005)

[2] AQA Physics A & B, EDEXCEL, OCR A & B, SQA Standard & Highers

[3] Stockholm Educational Air Shower Array – `http://www.particle.kth.se/SEASA/`

[4] Image courtesy of 'CMS Outreach' – `http://cmsinfo.cern.ch/`

[5] A Search for a Freonless Gas Mixture for Glass RPC, S. NARITA et al., IEEE Transac. on Nucl. Sci. 48 (2001) No. 3

[6] The Particle Detector BriefBook, R. K. BOCK and A. VASILESCU – `http://rkb.home.cern.ch/rkb/titleD.html`

[7] Wire Chamber Ageing, J. A. KADYK, Nucl. Inst. Meth. A 300 (1991) 436–479

[8] Wikipedia entry on cosmic rays, `http://en.wikipedia.org/wiki/Cosmic\_rays`

[9] A Thin Cosmic Rain, M. W. FRIEDLANDER, Harvard University Press (2000)

[10] North American Large-area Time Coincidence Arrays – `http://csr.phys.ualberta.ca/nalta/`

[11] HiRes website: `http://www.cosmic-ray.org/reading/detect.html`

[12] Cosmic Rays, A. W. WOLFENDALE, George Newnes Ltd. (1963)

[13] Cosmic Rays – S. Eidelman et al., Physics Letters B592, 1 (2004)

[14] Passage of Particles Through Matter – S. Eidelman et al., Physics Letters B592, 1 (2004)

[15] Detectors for Particle Radiation, K. KLEINKNECHT, Cambridge University Press (1998)

[16] Ionization Processes in Spark Disharge Plasmas, N. L. ALEKSANDROV and E. M. BAZELYAN, Plasma Sources Sci. Technol. 8 (1999) 285–294

[17] Resistive plate chamber with secondary electron emitters and microstrip readout, E. Ceron Zeballos et al. Nucl. Instr. Meth. in Phys. Res. A 392 (1997) 150–154

[18] Ionization Chambers & Counters, D. H. WILKINSON, Cambridge University Press

[19] Ageing and Recovering of s Glass RPC, A. CANDELA et al., Nucl. Instr. Meth. A 533 (2004) 116–120

[20] Resistive Cathode Transparency, G BATTISTONI et al., Nucl. Instr. Meth. 202 (1982) 459–464

[21] Thin Film Surface Resistivity, M. P. GUTIERREZ, H. LI, J. PATTON, `http://www2.sjsu.edu/faculty/selvaduray/page/papers/mate210/thinfilm.pdf`

[22] An Affordable Particle Detector for Education, J. Miles (2004)

[23] `http://www.cosmicrays.org/`

[24] Study of an Avalanche-mode Resistive Plate Chamber, J Ying et al. J. Phys. G: Nucl. Part. Phys. 26 (2000) page 1292

[25] Development of Resistive Plate Counters, R. SANTONICO and R. CARDARELLI, Nucl. Inst & Meth. 187 (1981) pages 377–380

[26] Particle Interaction notes, D. CUSSANS, Bristol University (2003)

[27] Cosmic Rays on the Pacific Ocean, A. H. COMPTON and R. N. TURNER, Phys. Rev. 52 (1937) 799 – 814

[28] Quenching Properties of Gas Mixture in Glass RPC Operated with Streamer Mode, M. KUMAGAI et al., Nucl. Instr. and Meth. A 533 (2004) 169–172

[29] Muon Stopping Power and Range Tables 10MeV – 100TeV, D. E. GROOM, N. V. MOKHOV and S. I. STRIGANOV, Atomic Data & Nucl. Data Tables 78 (2001) 183–356

[30] Test of Freonless Operation of Resistive Plate Chambers with Glas Electrodes – 1mm Gas Gap vs 2mm Gas Gap, H. SAKAUE, E. NAKANO, T. TAKAHASHI, Y. TERAMOTO, Nucl. Instr. Meth. A 482 (2002) 216–225

[31] Tables of Physical and Chemical Constants 16th Ed., G. W. KAYE, T. H. LABY (1996) Longman

[32] Wikipedia entry for Johnson noise – `http://en.wikipedia.org/wiki/Johnson\_noise`

[33] Spectar PETG Copolyester datasheet – `http://www.boedeker.com/spectar.htm`

[34] Electronics for Scientists, R. E. WEBB, (1990), Ellis Horwood